NATIONAL ADVISORY COMMITTEE FOR AERONAUTICS

TECHNICAL NOTE 3283

AERODYNAMIC FORCES, MOMENTS, AND STABILITY DERIVATIVES FOR SLENDER BODIES OF GENERAL CROSS SECTION

By Alvin H. Sacks

Ames Aeronautical Laboratory
Moffett Field, Calif.

NACA

Washington

November 1954

TABLE OF CONTENTS

TECHNICAL NOTE 3283

AERODYNAMIC FORCES, MOMENTS, AND STABILITY

DERIVATIVES FOR SLENDER BODIES OF

GENERAL CROSS SECTION

By Alvin H. Sacks

SUMMARY

The problem of determining the total forces, moments, and stability derivatives for a slender body performing slow maneuvers in a compressible fluid is treated within the assumptions of slender-body theory. General expressions for the total forces (except drag) and moments are developed in terms of the geometry and motions of the airplane, and formulas for the stability derivatives are derived in terms of the mapping functions of the cross sections.

All components of the motion are treated simultaneously and second derivatives as well as first are obtained, with respect to both the motion components and their time rates of change. Coupling of the longitudinal and lateral motions is thus automatically included. A number of general relationships among the various stability derivatives are found which are independent of the configuration, so that, at most, only 35 of a total of 325 first and second derivatives need be calculated directly. Calculations of stability derivatives are carried out for two triangular wings with camber and thickness, one with a blunt trailing edge, and for two wing-body combinations, one having a plane wing and vertical fin.

The influence on the stability derivatives of the squared terms in the pressure relation is demonstrated, and the apparent mass concept as applied to slender-body theory is discussed at some length in the light of the present analysis. It is shown that the stability derivatives can be calculated by apparent mass although the general expressions for the total forces and moments involve additional terms.

INTRODUCTION

Ever since R. T. Jones (ref. 1) in 1946 demonstrated the use of Munk's apparent mass concept of 1924 (ref. 2) for solving problems of slender wings in a compressible flow, an ever-increasing number of investigators have entered the field of analysis now commonly known as

slender-body theory. The stability derivatives of slender triangular
wings were treated by Ribner (ref. 3) in 1947 following the pattern of
Jones, and in 1948 Spreiter (ref. 4) extended the latter's result by
means of conformal mapping to include certain wing-body combinations.
Shortly thereafter, in 1949, Ward's general analysis for slender pointed
bodies in steady supersonic flow (ref. 5) was published.

After the appearance of Ward's analysis, a number of papers were
written on various aspects of slender-body theory including extensions
to subsonic flow and to "not-so-slender" bodies (e.g., refs. 6 and 7),
and in 1952 Phythian (ref. 8) developed an analysis which included time
variations in forward velocity and angles of incidence. Although many
papers (e.g., refs. 9 and 10) have been devoted to the calculation of
various stability derivatives for specific configurations, it is only in
the past few months that a report by Miles (ref. 11) has given the com-
plete counterpart of Ward's analysis for unsteady flow.

The determination of stability derivatives has long been of concern
to the engineer in connection with the dynamic behavior of airplanes,
but the problem has assumed even greater proportions in the more recent
slender configurations of missile design. The stability derivatives them-
selves correspond to the coefficients of a Taylor expansion representing
a particular component of force (say lift) or moment as a function of
the airplane motions. The coefficient of any particular motion (say q)
in the expansion is equal to the partial derivative of the force or
moment component with respect to that motion. Ordinarily, stability
derivatives are defined as these partial derivatives evaluated with all
of the independent variables except α set to zero, so that the usual
stability derivatives depend upon the initial angle of attack as well as
on the configuration. In the present paper, however, all derivatives
are evaluated with all of the independent variables (α, β, p, q, r, $\dot{\alpha}$, $\dot{\beta}$,
$\dot{p}$, $\dot{q}$, $\dot{r}$) set to zero. The advantages of this choice will become apparent
in the course of the analysis.

The present paper employs an approach believed to be novel in
slender-body theory and is concerned with developing formulas for the
forces and moments as well as the stability derivatives for general
slender wing-body combinations.[1] The significance of the squared terms
in the pressure relation for slender configurations precludes the
possibility of considering the longitudinal and lateral motions inde-
pendently, so all motions of the airplane are treated simultaneously.

---

[1]While the present analysis was being carried out, Bryson (ref. 12)
published a paper treating essentially the same subject from a different
viewpoint based on the tacit assumption that all the forces, moments,
and stability derivatives can be obtained from the apparent mass analogue.
This assumption and some of Bryson's results are discussed in a later
section.

The mathematical restrictions on the generality of the shapes that can be rigorously handled have been discussed in detail by Ward (ref. 5) and more recently for the unsteady case by Miles (ref. 11). Such discussion will not be repeated in this report.

LIST OF IMPORTANT SYMBOLS

a_n coefficient of $\dfrac{1}{\sigma^n}$ term in series expansion of the mapping function $\zeta = f(\sigma) = \sigma + \displaystyle\sum_{n=0}^{\infty} \dfrac{a_n}{\sigma^n}$

A_1 coefficient of $\dfrac{1}{\zeta}$ term in expansion of the complex potential $F(\zeta)$

A_{1_0} value of A_1 at $\alpha = \beta = p = q = r = 0$

B coefficient of $\ln \zeta$ in expansion of $F(\zeta)$; $B = \dfrac{U_0}{2\pi} \dfrac{dS}{dx}$

c_1 distance from airplane nose to pivot point

F complex potential $\varphi + i\psi$

l length of airplane

L force in the z direction (approximately lift)

L' rolling moment about the x axis

l_r reference length

M pitching moment about pivot point $x = c_1$

N yawing moment about pivot point $x = c_1$

p angular rolling velocity about the x axis

p_1 pressure

q angular pitching velocity about the y axis

q_r fluid speed relative to axes fixed in the body

q_n component of q_r normal to body contour in plane $x = $ const. (positive into the fluid)

q_s component of q_r tangential to body contour in plane $x = \text{const.}$ (positive counterclockwise looking upstream)

R $V + iW$

r angular yawing velocity about the z axis

r_0 radius of transformed circle corresponding to airplane cross section

S cross-sectional area

S_r reference area

t time

U_0 component of flight velocity along negative x axis

V_0 component of flight velocity along positive y axis

V $V_0 - r(x-c_1)$

V_1 speed of a point fixed in the xyz system of axes

u_r, v_r, w_r components of q_r in the x, y, z directions

W_0 component of flight velocity along positive z axis

W $W_0 - q(x-c_1)$

Y force in the y direction (side force)

xyz Cartesian coordinates fixed in the body (x rearward, y to starboard, z upward)

α angle of attack (angle between arbitrarily chosen xy plane and flight direction)

β angle of sideslip (angle between xz plane and flight direction)

θ angle between the positive y axis and the tangent to the body contour in a plane $x = \text{const.}$

ρ fluid mass density

ν outward normal to the body contour in plane $x = \text{const.}$

ζ $y + iz$

ζ_c complex coordinate of centroid of cross-sectional area
$(y_c + iz_c)$

σ complex coordinate in transformed circle plane

φ velocity potential

$\left.\begin{array}{l}\varphi_x, \varphi_y, \\ \varphi_z, \varphi_t\end{array}\right\}$ partial derivatives of φ with respect to x, y, z, and t

φ_2, φ_3 velocity potentials for unit velocity of the cross section in the y, z directions

φ' velocity potential associated with variations in shape and size of cross section with x

ψ stream function

ψ_s stream function along the contour of the cross section

Special Notations

$\oint$ contour integral taken once round the body cross section in the positive (counterclockwise) sense

Force coefficients: $C_Y = \dfrac{Y}{(1/2)\rho U_0^2 S_r}$, etc.

Moment coefficients: $C_m = \dfrac{M}{(1/2)\rho U_0^2 S_r l_r}$, etc.

Stability derivatives:

$$C_{Y_\alpha} = \frac{\partial C_Y}{\partial \alpha}; \qquad C_{Y_p} = \frac{\partial C_Y}{\partial \left(\dfrac{p l_r}{U_0}\right)}; \qquad C_{Y_{\alpha p}} = \frac{\partial^2 C_Y}{\partial \alpha\, \partial \left(\dfrac{p l_r}{U_0}\right)}$$

$$C_{Y_{\dot\alpha}} = \frac{\partial C_Y}{\partial \left(\dfrac{\dot\alpha l_r}{U_0}\right)}; \qquad C_{Y_{\dot p}} = \frac{\partial C_Y}{\partial \left(\dfrac{\dot p l_r^2}{U_0^2}\right)}; \qquad C_{Y_{pp}} = \frac{\partial^2 C_Y}{\partial \left(\dfrac{p l_r}{U_0}\right)^2}; \text{ etc.}$$

All derivatives are evaluated at

$$\alpha = \beta = p = q = r = \dot\alpha = \dot\beta = \dot p = \dot q = \dot r = 0$$

R   real part

I   imaginary part

$\dot{(\ )}$ derivative of ( ) with respect to time

$\bar{(\ )}$ complex conjugate of ( )

GENERAL ANALYSIS

The problem to be treated here is the determination of the aero-dynamic forces and moments (except drag) and the stability derivatives for a smooth slender airplane or missile of arbitrary cross section per-forming slow maneuvers in a compressible fluid. The configuration will be limited in that the base (if any) of the fuselage and all wing trail-ing edges must lie in a plane essentially normal to the longitudinal body axis.

Differential Equation and Pressure Relation

The linearized differential equation for the velocity potential of unsteady motion of a compressible fluid is the well-known wave equation

$$\frac{1}{c_0{}^2}\ \Phi_{\tau\tau}\ -\ \Phi_{\lambda\lambda}\ -\ \Phi_{\mu\mu}\ -\ \Phi_{\xi\xi}\ =\ 0 \tag{1}$$

where the system of axes $\lambda\mu\xi$ is fixed relative to the undisturbed fluid, c_0 is the speed of sound in the undisturbed fluid, and τ is time as measured in the $\lambda\mu\xi$ system. Thus the velocity potential Φ is express-ible as $\Phi = \Phi(\lambda,\mu,\xi,\tau)$.

In general, the pressure relation associated with the velocity potential Φ is given by (ref. 13, p. 19)

$$\frac{p_1}{\rho}\ =\ -\ \Phi_\tau\ -\ \frac{1}{2}\ q_1{}^2\ +\ \int\ p_1 d\left(\frac{1}{\rho}\right)\ +\ \text{const.} \tag{2}$$

where p_1 is pressure and q_1 is the magnitude of the fluid velocity expressible as[2]

$$q_1{}^2\ =\ \Phi_\lambda{}^2\ +\ \Phi_\mu{}^2\ +\ \Phi_\xi{}^2 \tag{3}$$

---

[2]The subscripts on p and q are used to distinguish them from the angular velocities of rolling and pitching.

It will be convenient for
the present problem to introduce
a coordinate system x_1yz which
is fixed in the airplane. The
axes chosen for this purpose are
shown in the sketch and comprise
a Cartesian coordinate system
endowed with the translational
velocities U_O, V_O, W_O and the
rotational velocities p, q, r
of the airplane. (Note that
this does not constitute a com-
pletely right-hand system.)
The x_1 axis passes through
the airplane nose, and the ori-
gin of the x_1yz system is
fixed at an arbitrary distance
c_1 from the nose as shown in
the sketch.
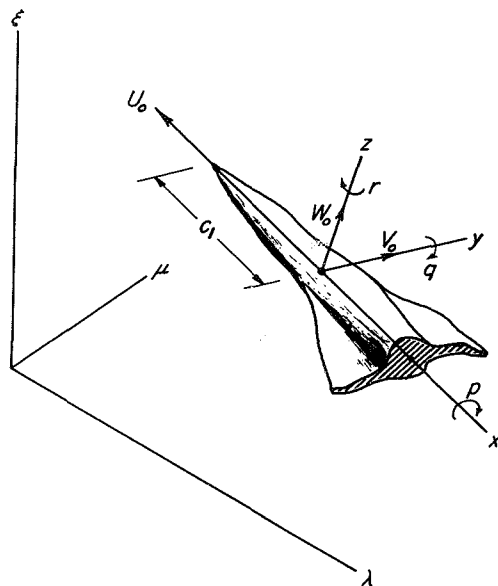
Since it is the purpose of this paper to study only instantaneous
forces and moments (i.e., no time histories), it will be sufficient to
choose an instant of time such that the positions of the moving x_1yz
system and the stationary $\lambda\mu\xi$ system are just coincident. Thus,
equations (1) and (2) will be expressed in the x_1yz system only for
this instant, designated $\tau = 0$. For this purpose a new function φ
is introduced such that

$$\varphi(x_1,y,z,t) = \Phi(\lambda,\mu,\xi,\tau) \tag{4}$$

Now, through the use of the transformations relating the moving and
stationary coordinates (see e.g., ref. 13, p. 12, and ref. 14, p. 79)
one finds at $\tau = t = 0$ that

$$\Phi_\tau = \frac{\partial\varphi}{\partial t}\frac{\partial t}{\partial \tau} + \frac{\partial\varphi}{\partial x_1}\frac{\partial x_1}{\partial \tau} + \frac{\partial\varphi}{\partial y}\frac{\partial y}{\partial \tau} + \frac{\partial\varphi}{\partial z}\frac{\partial z}{\partial \tau}$$

$$= \varphi_t + U_o\varphi_{x_1} - (V_o + pz - rx_1)\varphi_y - (W_o - py - qx_1)\varphi_z$$

and

$$\Phi_\lambda = \varphi_{x_1}; \qquad \Phi_\mu = \varphi_y; \qquad \Phi_\xi = \varphi_z$$

It can be seen from the sketch that the quantities $(V_o + pz - rx_1)$ and
$(W_o - py - qx_1)$ are simply the velocity components in the y and z
directions of a point fixed in the x_1yz system. Note that in the
corresponding x component $(-U_o + ry + qz)$ the products ry and qz
are considered negligible compared with U_o.

With the assumptions of slender bodies, small angles, and slow maneuvers, the differential equation (1) reduces to Laplace's equation in planes $x_1 = $ const. near the body; that is

$$\varphi_{yy} + \varphi_{zz} = 0 \tag{5}$$

It follows also that the density ρ must be treated as a constant in the pressure relation (2) which now becomes

$$\frac{p_1}{\rho} = -\Phi_\tau - \frac{1}{2}\left(\Phi_\mu{}^2 + \Phi_\xi{}^2\right) + \text{const.}$$

$$= -\varphi_t - U_o\varphi_{x_1} + (V_o + pz - rx_1)\varphi_y + (W_o - py - qx_1)\varphi_z -$$

$$\frac{1}{2}\left(\varphi_y{}^2 + \varphi_z{}^2\right) + \text{const.} \tag{6}$$

Here, for the sake of convention, one can transfer the origin of the moving axes to the body nose by letting

$$x_1 = x - c_1$$

so that pitching and yawing rotations are still made about an arbitrary pivot point $x = c_1$. Thus, introducing the notation

$$V = V_o - rx_1 = V_o - r(x - c_1)$$

$$W = W_o - qx_1 = W_o - q(x - c_1)$$

equation (6) can be written

$$\frac{p_1}{\rho} = -\varphi_t - U_o\varphi_x + (V + pz)\varphi_y + (W - py)\varphi_z - \frac{1}{2}\left(\varphi_y{}^2 + \varphi_z{}^2\right) + \text{const.} \tag{7}$$

This, then, is the pressure relation (referred to the moving body axes) upon which the calculations of the forces and moments will be based. It should be noted that a consistent application of the slenderness approximation requires the retention of the squared terms $\varphi_y{}^2$ and $\varphi_z{}^2$. Thus slender-body theory is not a strictly linear theory although the differential equation (5) is certainly linear. This means that solutions of equation (5) for φ (and hence the velocities) can be obtained by superposition, but the pressures cannot. Likewise, the forces and moments cannot be calculated by superposition except for those special cases in which the contribution of the squared terms to the loading vanishes. Furthermore, when the airplane is performing combined maneuvers (e.g., simultaneous rolling and pitching), the squared terms may contribute additional forces and moments. These in fact give rise to the second-order stability derivatives that will be included in the present analysis.

Total Forces and Moments

The analysis to be presented here
for calculating the total forces
(except drag) and moments on a slender
configuration will be the counterpart
of a method originally due to H. Blasius
(ref. 15) for obtaining the forces and
moments on a two-dimensional body of
arbitrary shape immersed in a steady
incompressible stream.[3] This analysis,
although not suited to the calculation
of total drag, will nevertheless take
proper account of the local forces
associated with leading-edge suction.
Consider a lamina of the slender air-
plane, cut parallel to the yz plane,
of thickness dx as shown in the sketch.
One can write immediately the differ-
ential lift and side force on an ele-
mental area in terms of the local
pressure p_1 on the body:
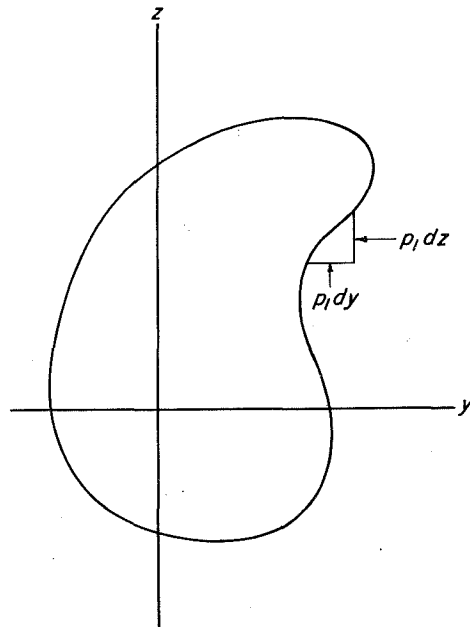
and

$$d^2L = p_1 \, dy \, dx$$

$$d^2Y = - p_1 \, dz \, dx$$

$$\left. \right\} \qquad (8)$$

Now, by introducing the complex variable $\zeta = y + iz$, one can express
the differential complex force as

$$d^2Y - i \, d^2L = - p_1 \, dz \, dx - i \, p_1 \, dy \, dx = - i \, p_1 \, dx \, d\bar{\zeta} \qquad (9)$$

where $\bar{\zeta}$ is the complex conjugate of ζ. In a similar fashion, the
differential rolling moment about the x axis can be expressed as

$$d^2L' = - p_1 \, z \, dz \, dx - p_1 \, y \, dy \, dx = - p_1 \, dx \, \mathbf{R}(\zeta d\bar{\zeta}) \qquad (10)$$

where $\mathbf{R}$ denotes the real part. Further, the differential yawing and
pitching moments about the pivot point $x = c_1$ are given by

$$d^2N - i \, d^2M = - (d^2Y - i \, d^2L) \, (x - c_1) = i \, p_1(x - c_1) \, dx \, d\bar{\zeta} \qquad (11)$$

Integration of equations (9), (10), and (11) gives for the total forces
and moments

[3]The method of Blasius has been extended to two-dimensional unsteady
incompressible flows by L. M. Milne-Thomson (ref. 16) and recourse will
be had to many of his techniques throughout the present analysis.

$$Y - iL = - i \int_0^l dx \oint p_1 \, d\bar{\zeta}$$

$$N - iM = i \int_0^l (x - c_1)dx \oint p_1 \, d\bar{\zeta} \qquad (12)$$

and

$$L' = - \mathbf{R} \int_0^l dx \oint p_1 \, \zeta d\bar{\zeta}$$

where the contour integrals are taken round the boundary of the airplane cross section in the positive (counterclockwise) sense. Before these integrations can be effected, the pressure p_1 must, of course, be expressed as a function of the complex variable ζ. Toward this end, it will be convenient to introduce two new definitions pertaining to velocities in the fixed and moving coordinate systems. First, the square of the speed of a point fixed in the xyz system can be written as

$$V_1{}^2 = U_0{}^2 + (V + pz)^2 + (W - py)^2 \qquad (13)$$

Second, it is noted that the square of the fluid speed relative to the xyz system is given by

$$q_r{}^2 = u_r{}^2 + v_r{}^2 + w_r{}^2 = (\varphi_x + U_0)^2 + (\varphi_y - V - pz)^2 + (\varphi_z - W + py)^2$$

$$(14)$$

so that, neglecting $\varphi_x{}^2$ in comparison with $\varphi_y{}^2$ and $\varphi_z{}^2$, one can write equation (7) in the form

$$\frac{p_1}{\rho} = - \varphi_t - \frac{1}{2} q_r{}^2 + \frac{1}{2} V_1{}^2 + \text{const.} \qquad (15)$$

This expression will now be formed as a function of ζ through the introduction of the complex variable $R = V + iW$ and the complex potential $F = \varphi + i\psi$.

The speed V_1 is immediately expressible as

$$V_1{}^2 = U_0{}^2 + \left[(V + pz) + i(W - py)\right]\left[(V + pz) - i(W - py)\right]$$

$$= U_0{}^2 + (R - ip\zeta)(\bar{R} + ip\bar{\zeta}) \qquad (16)$$

while the components v_r and w_r of the relative fluid velocity are related to F through the complex velocity by
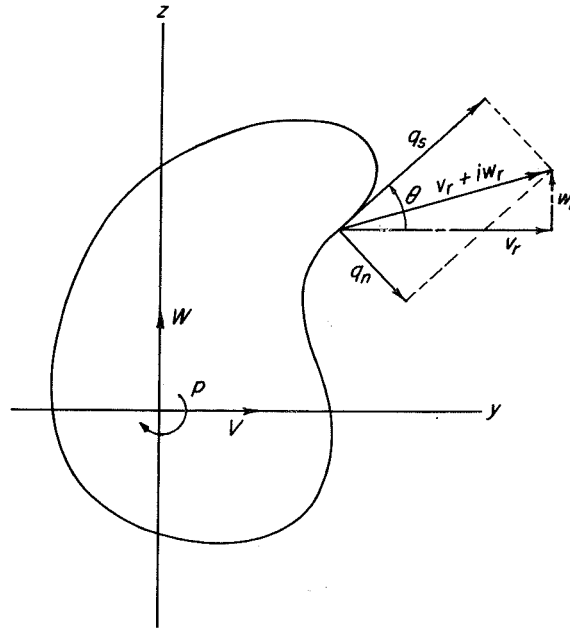
$$v_r - iw_r = \frac{dF}{d\zeta} - (V + pz) + i(W - py) = \frac{dF}{d\zeta} - \bar{R} - ip\bar{\zeta} \qquad (17)$$

Furthermore, at the body sur-
face it will be seen from the
sketch that

$$v_r + iw_r = q_s e^{i\theta} +$$

$$q_n e^{-i\left(\frac{\pi}{2} - \theta\right)}$$

$$= (q_s - iq_n)e^{i\theta}$$

so that

$$v_r - iw_r = (q_s + iq_n)e^{-i\theta}$$

$$(18)$$

where q_s and q_n are the
tangential and normal com-
ponents of the transverse
relative velocity and θ is the angle defined in the sketch. Com-
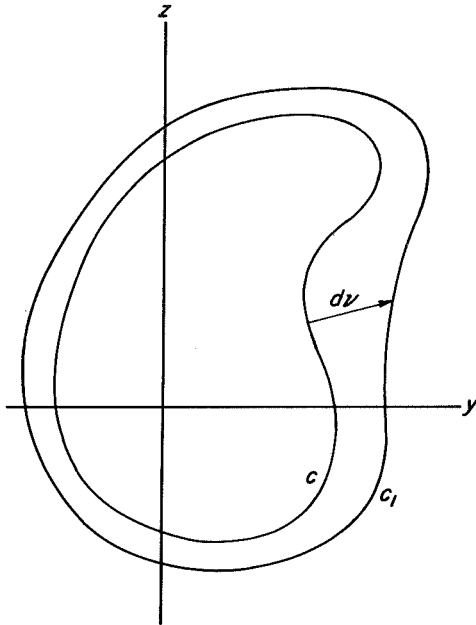parison of equations (17) and (18) gives

$$q_s + iq_n = \left(\frac{dF}{d\zeta} - \bar{R} - ip\bar{\zeta}\right)e^{i\theta} \qquad (19)$$

from which

$$q_s{}^2 = \left(\frac{dF}{d\zeta} - \bar{R} - ip\bar{\zeta}\right)^2 e^{2i\theta} - 2iq_n\left(\frac{dF}{d\zeta} - \bar{R} - ip\bar{\zeta}\right)e^{i\theta} - q_n{}^2$$

It is now noted that (see sketch above)

$$v_r{}^2 + w_r{}^2 = q_s{}^2 + q_n{}^2 = q_r{}^2 - U_o{}^2 - 2U_o\varphi_x$$

$$= \left(\frac{dF}{d\zeta} - \bar{R} - ip\bar{\zeta}\right)^2 e^{2i\theta} - 2iq_n\left(\frac{dF}{d\zeta} - \bar{R} - ip\bar{\zeta}\right)e^{i\theta} \qquad (20)$$

Finally, the boundary condition at the body surface requires that the normal component of the fluid velocity relative to the moving xyz system be equal to the normal component of the forward flight velocity. Let C be the contour of the airplane cross section in the plane x = const. and let C_1 represent the projection on that plane of the contour at x + dx (see sketch). If ν is the outward normal to C at any point, and $d\nu$ is the distance between C and C_1 measured along the normal, then the above boundary condition is, to the present order of accuracy,

$$q_n = U_o \frac{d\nu}{dx} \qquad (21)$$

Thus the pressure relation of equation (15) can now be written (for points on the airplane surface) in the desired form

$$\frac{p_1}{\rho} = - \varphi_t - U_o \varphi_x - \frac{1}{2}\left(\frac{dF}{d\zeta} - \overline{R} - ip\overline{\zeta}\right)^2 e^{2i\theta} + iU_o \frac{d\nu}{dx}\left(\frac{dF}{d\zeta} - \overline{R} - ip\overline{\zeta}\right) e^{i\theta} +$$

$$\frac{1}{2}(R - ip\zeta)(\overline{R} + ip\overline{\zeta}) + \text{const.} \qquad (22)$$

Reduction of the integrals.- Before making use of equation (22) in writing the integrals for the forces and moments, it will be useful to notice from the sketch on page 11 that the differential distances on the body contour in planes x = const. are related by the angle θ so that dy = ds cos θ and dz = ds sin θ where ds is the differential arc length, positive counterclockwise. Hence,

$$d\zeta = ds\, e^{i\theta}; \qquad d\overline{\zeta} = ds\, e^{-i\theta}; \qquad d\overline{\zeta} = d\zeta\, e^{-2i\theta} \qquad (23)$$

so that the first integral of equation (12) for the complex lateral force can be written, after expanding the squared term in the pressure relation, in the form

$$Y - iL = i\rho \int_0^l dx \oint \varphi_t d\overline{\zeta} + i\rho U_o \int_0^l dx \oint \varphi_x d\overline{\zeta} +$$

$$i \frac{\rho}{2} \int_0^l dx \oint \left(\frac{dF}{d\zeta}\right)^2 d\zeta + i \frac{\rho}{2} \int_0^l dx \oint (\overline{R} + ip\overline{\zeta})^2 d\zeta -$$

$$i\rho \int_0^l \overline{R} \, dx \oint \frac{dF}{d\zeta} d\zeta + \rho p \int_0^l dx \oint \overline{\zeta} \frac{dF}{d\zeta} d\zeta +$$

$$\rho U_o \int_0^l dx \oint \frac{d\nu}{dx} \frac{dF}{d\zeta} ds - \rho U_o \int_0^l dx \oint \frac{d\nu}{dx} (\overline{R} + ip\overline{\zeta}) ds -$$

$$i \frac{\rho}{2} \int_0^l dx \oint (R - ip\zeta) (\overline{R} + ip\overline{\zeta}) d\overline{\zeta} \tag{24}$$

Note that the constant term in the pressure relation contributes nothing to the contour integrals of equation (12).

The nine contour integrals of equation (24) can be divided into three types: (a) integrals that do not depend on the velocity potential; (b) integrals containing the real potential φ; and (c) integrals containing the complex potential F. The first type can be integrated at once and these will be dealt with first. The second type will be reduced to integrals of the third type by determining the stream function on the boundary, and the third type will then be handled by the method of residues.

It is first noted that $\oint \frac{d\nu}{dx} ds$ is simply the rate of change of

cross-sectional area S and that $\oint \overline{\zeta} \frac{d\nu}{dx} ds$ is the complex conjugate

of the rate of change (in the x direction) of the moment of cross-sectional area. Thus, one can write

$$\oint \frac{d\nu}{dx} (\overline{R} + ip\overline{\zeta}) ds = \overline{R} \frac{dS}{dx} + ip \frac{d}{dx} (S\overline{\zeta}_c) \tag{25}$$

where $\overline{\zeta}_c$ is the complex conjugate of the position of the centroid of area of the cross section.

The other two integrals of equation (24) that do not depend on the velocity potential can be conveniently evaluated by the use of Stokes' theorem which can be stated in complex form as (see ref. 16, p. 130)

or
$$\oint f(\zeta,\overline{\zeta})d\zeta = 2i \iint_S \frac{\partial f}{\partial \overline{\zeta}} dS$$
$$\oint f(\zeta,\overline{\zeta})d\overline{\zeta} = -2i \iint_S \frac{\partial f}{\partial \zeta} dS$$

(26)

where S is the area enclosed by the contour. Thus, using the first form of equation (26), one can write

$$\oint (\overline{R} + ip\overline{\zeta})^2 d\zeta = 2i \iint_S 2ip(\overline{R} + ip\overline{\zeta})dS = -4pS(\overline{R} + ip\overline{\zeta}_c) \quad (27)$$

where S is the airplane cross-sectional area. Similarly, from the second form of equation (26),

$$\oint (R - ip\zeta)(\overline{R} + ip\overline{\zeta})d\overline{\zeta} = -2pS(\overline{R} + ip\overline{\zeta}_c) \quad (28)$$

Thus, all the integrals of the first type discussed above have been evaluated.

Before introducing the stream function for the evaluation of the first two integrals of equation (24), it is well to note that the time differentiation can be taken outside the integral sign with no difficulty, but the x differentiation cannot since the contour of integration is itself a function of x. It is shown in Appendix A that

$$\oint \varphi_x d\overline{\zeta} = \frac{\partial}{\partial x} \oint \varphi d\overline{\zeta} - \int_C \varphi_z \frac{\partial Z_1}{\partial x} dy + i \int_C \varphi_y \frac{\partial Y_1}{\partial x} dz$$

where C is the contour of integration round the airplane cross section and the surface of the airplane can be expressed either as

$$z = Z_1(x,y)$$

or

$$y = Y_1(x,z)$$

Corresponding to these expressions for the surface are the expressions for the slopes of the surface

$$\frac{\partial Z_1}{\partial x} = -\frac{d\nu/dx}{\cos\theta}$$

and

$$\frac{\partial Y_1}{\partial x} = \frac{d\nu/dx}{\sin\theta}$$

so that, recalling the relations
of equations (23), one can write

$$\oint \varphi_x d\bar{\zeta} = \frac{\partial}{\partial x} \oint \varphi d\bar{\zeta} +$$

$$\oint \frac{d\nu}{dx} (\varphi_z + i\varphi_y) ds$$

$$= \frac{\partial}{\partial x} \oint \varphi d\bar{\zeta} + i \oint \frac{d\nu}{dx} \frac{dF}{d\zeta} ds$$

$$(29)$$

Now, in order to express the

required integral $\oint \varphi d\bar{\zeta}$ in terms

of the complex potential through
the relation $\varphi = \bar{F} + i\Psi$, the stream
function on the boundary will be
obtained from the boundary condition
of equation (21). That is, the
total outward normal of the fluid velocity in the plane $x = const.$ is
given by the sum of q_n and the normal velocity of a point on the
boundary considered fixed in the xyz system. Hence, (see sketch),
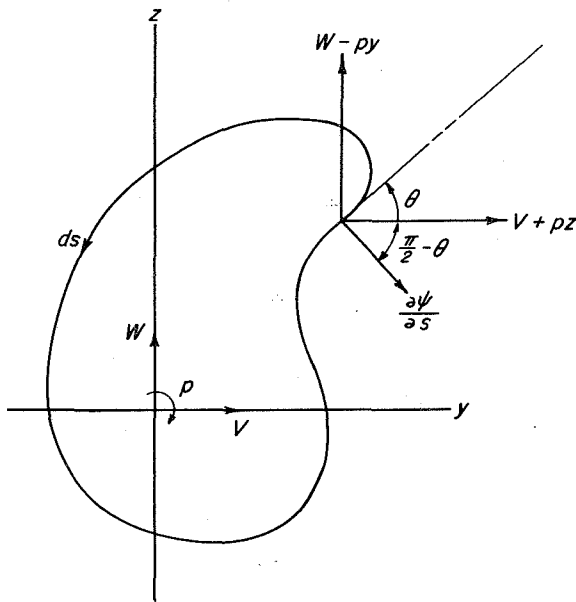
$$\frac{\partial \Psi}{\partial s} = (V + pz)\sin \theta - (W - py)\cos \theta + U_o \frac{d\nu}{dx} \tag{30}$$

and it is recalled that $\sin \theta = dz/ds$ and $\cos \theta = dy/ds$. The sense
of ds is indicated by the arrow along the contour. Thus, integrating
along the contour, one finds that the stream function on the surface is
given by

$$\Psi_s = Vz + \frac{1}{2} pz^2 - Wy + \frac{1}{2} py^2 + U_o \int \frac{d\nu}{dx} ds + G(x,t)$$

where $G(x,t)$ is an arbitrary function of x and t. Now Ψ_s can also
be expressed as a function of the complex variables ζ and R by noting
that

$$\mathbf{I}(\bar{R}\zeta) = Vz - Wy = -\frac{1}{2} (\bar{R}\zeta - R\bar{\zeta})$$

and

$$y^2 + z^2 = \zeta\bar{\zeta}$$

whence

$$\Psi_s = -\frac{i}{2}(\overline{R}\zeta - R\overline{\zeta}) + \frac{1}{2}p\zeta\overline{\zeta} + U_o\int\frac{d\nu}{dx}\,ds + G(x,t) \tag{31}$$

The integral $\oint \varphi\,d\overline{\zeta}$ is now expressible in terms of the complex potential since $\varphi = \overline{F} + i\Psi$ and the integral $\oint \Psi\,d\overline{\zeta}$ can be evaluated from equation (31). That is, if one sets $\Psi = \Psi_o + \Psi_1$ where Ψ_1 represents the integral term of equation (31), then

$$\oint \Psi\,d\overline{\zeta} = \oint \Psi_o\,d\overline{\zeta} + \oint \Psi_1\,d\overline{\zeta} = \oint \Psi_o\,d\overline{\zeta} + [\Psi_1\overline{\zeta}]_C - \oint \overline{\zeta}\,d\Psi_1 \tag{32}$$

Now, Ψ_1 taken once round the contour has the value $U_o\oint\frac{d\nu}{dx}\,ds$ or simply $U_o\frac{dS}{dx}$ and it is recalled that $\oint \overline{\zeta}\frac{d\nu}{dx}\,ds = \frac{d}{dx}(S\overline{\zeta}_c)$, so that upon evaluating $\oint \Psi_o\,d\overline{\zeta}$ by the second form of Stokes' theorem (eq. (26)) and noting that $\oint G(x,t)\,d\overline{\zeta} = 0$, one finds

$$\oint \Psi\,d\overline{\zeta} = -S(\overline{R} + ip\overline{\zeta}_c) + U_o\overline{\zeta}_o\frac{dS}{dx} - U_o\frac{d}{dx}(S\overline{\zeta}_c) \tag{33}$$

where $\overline{\zeta}_o$ is the complex conjugate of the point at which the integration was begun on the boundary. The final expression for $\oint \varphi\,d\overline{\zeta}$ is therefore

$$\oint \varphi\,d\overline{\zeta} = \oint \overline{F}\,d\overline{\zeta} + i\oint \Psi\,d\overline{\zeta} = \oint \overline{F}\,d\overline{\zeta} + iU_o\overline{\zeta}_o\frac{dS}{dx} - iS(\overline{R} + ip\overline{\zeta}_c) - iU_o\frac{d}{dx}(S\overline{\zeta}_c) \tag{34}$$

and the time derivative is

$$\oint \varphi_t\,d\overline{\zeta} = \frac{\partial}{\partial t}\oint \varphi\,d\overline{\zeta} = \frac{\partial}{\partial t}\oint \overline{F}\,d\overline{\zeta} - iS\frac{\partial\overline{R}}{\partial t} \tag{35}$$

Of the remaining integrals in equation (24) there is one which still requires modification before the method of residues can be applied. Specifically, since $F = \bar{F} + 2i\Psi$ one can write

$$\oint \bar{\zeta} \, dF = \oint \bar{\zeta}(d\bar{F} + 2i \, d\Psi) = \oint \bar{\zeta} \, d\bar{F} + 2i \oint \bar{\zeta} \, d\Psi$$

and the second integral can be integrated by parts using equation (33) and noting that Ψ taken once round the contour has the value $U_0 \dfrac{dS}{dx}$. The resulting expression is

$$\oint \bar{\zeta} \, dF = \oint \bar{\zeta} \, d\bar{F} + 2iS(\bar{R} + ip\bar{\zeta}_c) + 2iU_0 \frac{d}{dx}(S\bar{\zeta}_c) \tag{36}$$

so that equation (24) for the complex force can finally be written (after collection and cancellation of terms) in the form

$$Y - iL = i\rho \int_0^l dx \frac{\partial}{\partial t} \oint \bar{F} \, d\bar{\zeta} + \rho \int_0^l S \frac{\partial \bar{R}}{\partial t} \, dx + i\rho U_0 \oint_{x=l} \bar{F} \, d\bar{\zeta} -$$

$$i\rho U_0 \oint_{x=0} \bar{F} \, d\bar{\zeta} - \rho U_0 \left[U_0 \bar{\zeta}_0 \frac{dS}{dx} - S(\bar{R} + 2ip\bar{\zeta}_c) - U_0 \frac{d}{dx}(S\bar{\zeta}_c) \right]_{x=l} +$$

$$i \frac{\rho}{2} \int_0^l dx \oint \left(\frac{dF}{d\zeta} \right)^2 d\zeta - \rho U_0 \int_0^l \bar{R} \frac{dS}{dx} \, dx - i\rho \int_0^l \bar{R} \, dx \oint dF +$$

$$\rho p \int_0^l dx \oint \bar{\zeta} \, d\bar{F} + i\rho p \int_0^l S(\bar{R} + ip\bar{\zeta}_c) \, dx \tag{37}$$

It should be pointed out that several terms have vanished by virtue of the fact that the x axis passes through the airplane nose. In particular, note that $S = \bar{\zeta}_c = 0$ at $x = 0$.

The complex potential.- Although equation (37) appears quite unwieldy, all of the contour integrals are now in a form which admits of evaluation by the method of residues. For a body moving through still air, as in the present problem, all velocities vanish at infinity and the complex potential F can be expanded in a Laurent series of the form

$$F = B(x) \ln \zeta + \sum_{n=1}^{\infty} \frac{A_n(x,t)}{\zeta^n} + D(x,t) \tag{38}$$

where $B(x)$ is a source strength and the coefficients $A_n(x,t)$ give the intensities of all the higher order singularities representing the desired body shape and motions. This expansion applies only for large values of ζ, but since there are no singularities outside the body, the contour integrals can be evaluated around a contour sufficiently large to insure the validity of the expansion. The arbitrary function $D(x,t)$ is of no concern here since it can contribute nothing to the contour integrations. For the determination of drag, on the other hand, this function would be required.

From equation (38), the derivative of F is

$$\frac{dF}{d\zeta} = \frac{B}{\zeta} - \sum_{n=1}^{\infty} \frac{nA_n}{\zeta^{n+1}}$$

so that

$$\left(\frac{dF}{d\zeta}\right)^2 = \frac{B^2}{\zeta^2} - \frac{2B}{\zeta} \sum_{n=1}^{\infty} \frac{nA_n}{\zeta^{n+1}} + \left(\sum_{n=1}^{\infty} \frac{nA_n}{\zeta^{n+1}}\right)^2$$

Now it is seen that the residue of $(dF/d\zeta)^2$ is zero since there is no $1/\zeta$ term in the expansion. Therefore,

$$\oint \left(\frac{dF}{d\zeta}\right)^2 d\zeta = 2\pi i \ \mathrm{Res}\left(\frac{dF}{d\zeta}\right)^2 = 0 \tag{39}$$

Also

$$\oint dF = \oint \frac{dF}{d\zeta} \, d\zeta = 2\pi i \ \mathrm{Res}\left(\frac{dF}{d\zeta}\right) = 2\pi i B \tag{40}$$

Similarly, if one writes the conjugate function

$$\overline{F} = \overline{B}(x) \ln \overline{\zeta} + \sum_{n=1}^{\infty} \frac{\overline{A}_n(x,t)}{\overline{\zeta}^n} + \overline{D}(x,t) \tag{41}$$

it follows that

$$\oint \overline{F} d\overline{\zeta} = -2\pi i \overline{B}\overline{\zeta}_0 - 2\pi i \overline{A}_1 \tag{42}$$

and

$$\oint \overline{\zeta} d\overline{F} = \oint \overline{\zeta} \frac{d\overline{F}}{d\overline{\zeta}} \, d\overline{\zeta} = -2\pi i \ \mathrm{Res}\left(\overline{\zeta} \frac{d\overline{F}}{d\overline{\zeta}}\right) = +2\pi i \overline{A}_1 \tag{43}$$

The coefficient B (and, hence, $\overline{B}$) can be evaluated by calculating the

integral $\oint \dfrac{\partial \varphi}{\partial n} \, ds$ in two different ways. Thus

$$\oint \frac{\partial \varphi}{\partial n} \, ds = \oint \frac{\partial \psi}{\partial s} \, ds = [\psi]_C = U_o \oint \frac{d\nu}{dx} \, ds = U_o \frac{dS}{dx}$$

and, by virtue of Gauss' theorem,

$$\oint \frac{\partial \varphi}{\partial n} \, ds = \int_0^{2\pi} \left(\frac{\partial \varphi}{\partial r} \right)_{r=r_1} r_1 d\theta = \int_0^{2\pi} \frac{B}{r_1} \, r_1 d\theta = 2\pi B$$

where r_1 is the radius of a circle enclosing the body cross section.
Hence, it is seen that

$$B = \overline{B} = \frac{U_o}{2\pi} \frac{dS}{dx} \tag{44}$$

The final expression for the complex lateral force is obtained by
using equations (39) to (44) in rewriting equation (37). That is,

$$Y - iL = 2\pi\rho U_o \overline{A}_{1_{x=l}} + \rho U_o \left[S(\overline{R} + 2ip\overline{\zeta}_c) + U_o \frac{d}{dx}(S\overline{\zeta}_c) \right]_{x=l} +$$

$$2\pi\rho \int_0^l \frac{\partial \overline{A}_1}{\partial t} \, dx + \rho \int_0^l S \frac{\partial \overline{R}}{\partial t} \, dx + 2\pi i \rho p \int_0^l \overline{A}_1 dx +$$

$$i\rho p \int_0^l S(\overline{R} + ip\overline{\zeta}_c) dx \tag{45}$$

For the case of steady straight flight $\left(\dfrac{\partial \overline{A}_1}{\partial t} = \dfrac{\partial \overline{R}}{\partial t} = p = 0 \right)$, the complex

force of equation (45) reduces to that given by Ward (ref. 5). Although
equation (45) applies to slender airplanes having cross sections of
arbitrary shape, it is of interest that in a large number of practical
cases, it is possible to choose the x axis so as to place the center
of cross-sectional area always along the axis and thus to make $\overline{\zeta}_c$
equal to zero. The simplest example would be an airplane having mirror
symmetry of area about both the y and z axes. If the wings have no
thickness, this places no restriction on the wings themselves with regard
to number of wings, arrangement, dihedral, camber, etc. Equation (45)

as it stands gives the total side force and lift on a slender configuration having a nose at the forward end. However, it can also be used to give the contribution to these forces of a segment of the airplane lying between the planes $x = l_1$ and $x = l_2$ by simply evaluating $Y - iL$ for $l = l_1$ and $l = l_2$ and subtracting the results.

If one considers the transformation of the arbitrary cross section in the ζ plane to a circle in the σ plane

$$\zeta = f(\sigma) = \sigma + \sum_{n=0}^{\infty} \frac{a_n}{\sigma^n} \tag{46}$$

it can be shown (see Appendix B) that the dependence of the residue A_1 (and, hence, $\overline{A_1}$) on the rolling velocity p is determined by the form of $f(\sigma)$ and therefore by the shape of the airplane cross section. It is found that A_1 is independent of p if a_0 vanishes and if $f(\sigma)$ contains either only odd negative powers of σ (n odd) or else only even negative powers of σ (n even). It can be seen that if n is odd then $f(-\sigma) = -f(\sigma)$ and, hence, the cross section has symmetry about two orthogonal axes. The statement can therefore be made that for airplanes having symmetry about both the y and z axes (no dihedral) one can determine the total complex force if he knows only the complex potential due to pure translation in the yz plane.

An expression for the pitching and yawing moments can now be obtained from equation (12) by a procedure exactly parallel to that used in obtaining equation (45). Making use of the foregoing evaluations of the required contour integrals, one finds that the resulting expression is

$$N - iM = -2\pi\rho U_0 \int_0^l (x - c_1) \frac{\partial \overline{A_1}}{\partial x} dx - \rho U_0 \int_0^l (x - c_1) \frac{\partial}{\partial x} \left[S(\overline{R} + 2ip\overline{\zeta}_c) + \right.$$

$$\left. U_0 \frac{d}{dx} (S\overline{\zeta}_c) \right] dx - 2\pi\rho \int_0^l (x - c_1) \frac{\partial \overline{A_1}}{\partial t} dx - \rho \int_0^l (x - c_1)S \frac{\partial \overline{R}}{\partial t} dx -$$

$$2\pi i\rho p \int_0^l (x - c_1)\overline{A_1} dx - i\rho p \int_0^l (x - c_1) (\overline{R} + ip\overline{\zeta}_c)S \, dx \tag{47}$$

The evaluation of the integrals for the rolling moment L' is somewhat different due to the additional ζ appearing in the expression of equation (12), so that the integrand of some of the contour integrals appearing here will be nonanalytic in the variable of integration. This precludes a direct application of the method of residues. Such an

integral, which does, in fact, arise is $\mathbf{I} \oint \zeta \overline{\zeta} dF$. However, in this instance it can be shown with the aid of equations (26) and (31) that

$$\mathbf{I} \oint \zeta \overline{\zeta} dF = \oint \zeta \overline{\zeta} d\Psi = 2S\mathbf{R}(\overline{R}\zeta_c) + U_o \oint \zeta \overline{\zeta} \frac{d\nu}{dx} ds \qquad (48)$$

Evaluation of other required contour integrals by means of equations (26), (31), and (38) yields

$$\left. \begin{array}{l} \mathbf{R} \oint \left(\frac{dF}{d\zeta}\right)^2 \zeta d\zeta = 0 \\[4mm] \oint \zeta \, dF = - 2\pi i A_1 \end{array} \right\} \qquad (49)$$

and it can be shown in a manner parallel to that of Appendix A that

$$\mathbf{R} \oint \varphi_x \zeta d\overline{\zeta} = \mathbf{R}\left(\frac{\partial}{\partial x} \oint \varphi \zeta d\overline{\zeta} \right) - \mathbf{I} \oint \frac{d\nu}{dx} \frac{dF}{d\zeta} \zeta ds \qquad (50)$$

so that the final expression for the rolling moment can be written in the form

$$L' = \rho U_o \mathbf{R} \oint_{x=l} \varphi \zeta d\overline{\zeta} + \rho \mathbf{R} \int_o^l dx \frac{\partial}{\partial t} \oint \varphi \zeta d\overline{\zeta} - 2\pi \rho \, \mathbf{I} \int_o^l \overline{R} A_1 dx -$$

$$\rho p \mathbf{R} \int_o^l S(R\overline{\zeta}_c - 2\overline{R}\zeta_c) dx - \rho U_o \mathbf{I} \int_o^l \overline{R} \frac{d}{dx} (S\zeta_c) dx \qquad (51)$$

or, since $\mathbf{R}(\zeta d\overline{\zeta}) = \frac{1}{2} d(\zeta \overline{\zeta})$,

$$L' = \frac{1}{2} \rho U_o \mathbf{R} \oint_{x=l} F d(\zeta \overline{\zeta}) + \frac{1}{2} \rho \mathbf{R} \int_o^l dx \frac{\partial}{\partial t} \oint F d(\zeta \overline{\zeta}) - 2\pi \rho \mathbf{I} \int_o^l \overline{R} A_1 dx -$$

$$\rho p \mathbf{R} \int_o^l S(R\overline{\zeta}_c - 2\overline{R}\zeta_c) dx - \rho U_o \mathbf{I} \int_o^l \overline{R} \frac{d}{dx} (S\zeta_c) dx \qquad (52)$$

page 22 NACA TN 3283

In the case of configurations possessing mirror symmetry about both the y and z axes (no dihedral), the general expression of equation (51) can be greatly simplified. If one writes for such a case

$$\varphi = V\varphi_2 + W\varphi_3 + p\varphi_4 + \varphi'$$

where φ_2 and φ_3 represent pure translations along the y and z axes, φ_4 is a pure rotation about the x axis, and φ' is associated with the variation of cross section with x, it can be shown from symmetry considerations that

$$\mathbf{R} \oint \varphi_2 \zeta \, d\bar{\zeta} = \mathbf{R} \oint \varphi_3 \zeta \, d\bar{\zeta} = \mathbf{R} \oint \varphi' \zeta \, d\bar{\zeta} = 0$$

Hence,

$$\mathbf{R} \oint \varphi \zeta \, d\bar{\zeta} = p\mathbf{R} \oint \varphi_4 \zeta \, d\bar{\zeta}$$

and, since φ_4 is the potential due to pure rotation about the x axis, it follows that

$$\mathbf{R} \left(\frac{\partial}{\partial t} \oint \varphi \zeta \, d\bar{\zeta} \right) = 0$$

Therefore, recalling that $\zeta_c = 0$ for configurations having symmetry about the y and z axes, one finds that the general expression of equation (51) reduces to

$$L' = \rho U_0 p \mathbf{R} \oint_{x=l} \varphi_4 \zeta \, d\bar{\zeta} - 2\pi\rho \mathbf{I} \int_0^l \bar{R} A_1 dx \qquad (53)$$

and it has already been pointed out that for these cases A_1 is independent of the rolling velocity p. Thus, for symmetrical configurations, the rolling moment has now been expressed as the sum of two independent parts, one due to pure rolling and one due to pure translation.

STABILITY DERIVATIVES

The specific maneuvers to be considered here will now be defined so that stability derivatives can be determined. Rotations are performed about the xyz (body) axes[4] at an attitude defined by the angles of

----

[4]Rolling about the wind axis can be treated as a special case by the proper choice of the arbitrary body axes.

attack and sideslip at $t = 0$, and
accelerations are permitted in the
fixed vertical and horizontal
planes. In particular, if the
angles of attack and sideslip at
$t = 0$ are denoted by α_O and β_O,
respectively, then the velocities
V and W at any time t are given
by (see sketch)

$$V = U_O\beta_O\cos pt +$$

$$U_O\alpha_O\sin pt - r(x - c_1)$$

$$W = - U_O\alpha_O\cos pt +$$
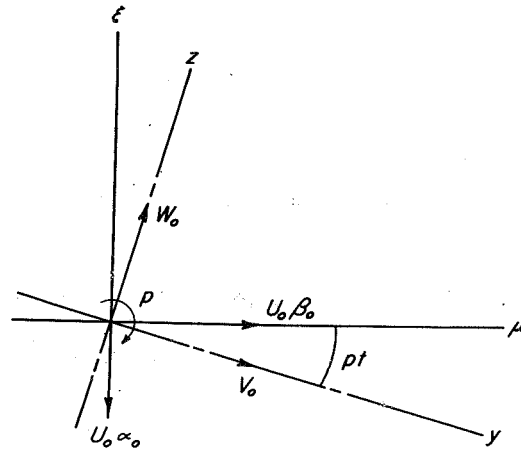
$$U_O\beta_O\sin pt - q(x - c_1)$$

From these expressions one finds that

$$\overline{R} = V - iW = (U_O\beta_O + iU_O\alpha_O)e^{-ipt} - (r - iq)(x - c_1)$$

and

$$\frac{\partial\overline{R}}{\partial t} = - ip(U_O\beta_O + iU_O\alpha_O)e^{-ipt} + e^{-ipt}(U_O\dot\beta_O + iU_O\dot\alpha_O) -$$

$$(\dot r - i\dot q)(x - c_1) - it\dot p(U_O\beta_O + iU_O\alpha_O)e^{-ipt}$$

It will be noticed that in the above expressions, the velocity U_O (along
the x axis) is considered constant. This means that pure pitching and
yawing motions ($q, r \neq 0$) are performed at constant angles of attack and
sideslip, so that for such maneuvers the airplane follows a curved flight
path. Now, setting $t = 0$ in the above expressions, one finds

$$\overline{R} = U_O\beta + iU_O\alpha - (r - iq)(x - c_1)$$

and

$$\frac{\partial\overline{R}}{\partial t} = U_O\dot\beta + iU_O\dot\alpha - ip(U_O\beta + iU_O\alpha) - (\dot r - i\dot q)(x - c_1) \qquad (54)$$

and these relations can be substituted directly into equations (45), (47),
and (51) for the forces and moments. It will be noted that the subscript
on $\dot\alpha$ and $\dot\beta$ has been dropped. This means that for the rolling case
($p \neq 0$) $\dot\alpha$ and $\dot\beta$ of equation (54) are not the time rates of change of the
actual angles of attack and sideslip since $\dot\alpha$ and $\dot\beta$ are measured in the

fixed vertical and horizontal planes. The alternative would have been
to define $\dot{\alpha}$ and $\dot{\beta}$ as the actual rates of change of α and β (i.e.,
$\dot{\alpha} = \dot{\alpha}_0 - \beta p$ and $\dot{\beta} = \dot{\beta}_0 + \alpha p$ at $t = 0$) in which case the coupling of
p with α and β would be obscured by the definition. This would lead,
for example, to a nonzero value of $\dot{\alpha} C_{m_{\dot{\alpha}}}$ when the maneuver consists of
pure rolling at an initial angle of sideslip. This seems undesirable.

In seeking stability derivatives for the general problem under con-
sideration, it will be advantageous to employ the transformation of the
airplane cross section to the circle (see Appendix B). In this way, it
will be possible to carry out differentiations of the forces and moments
explicitly with respect to the airplane motions and thus obtain the
stability derivatives in terms of the transformation without specifying
the complex potential. Thus, from Appendix B,

$$\overline{A}_1 = R\overline{a}_1 - \overline{R}r_0^2 - ip\left(\overline{a}_0 r_0^2 + \overline{a}_1 a_0 + \frac{\overline{a}_2 a_1}{r_0^2} + \frac{\overline{a}_3 a_2}{r_0^4} + \ldots\right) + \overline{A}_{1_0}$$

(55)

and therefore

$$\frac{\partial \overline{A}_1}{\partial t} = \overline{a}_1 \frac{\partial R}{\partial t} - r_0^2 \frac{\partial \overline{R}}{\partial t} - i\dot{p}(\overline{a}_0 r_0^2 + \overline{a}_1 a_0 + \ldots)$$

(56)

where a_1 is the coefficient of the $1/\sigma$ term of the mapping function
and r_0 is the radius of the transformed circle. It is recalled that,
as shown in Appendix B, $\overline{A}_{1_0}$ is simply the value of $\overline{A}_1$ at $\alpha = \beta = p =$
$q = r = 0$ and is therefore directly associated with the shape of the con-
figuration and the choice of axes.

The stability derivatives will be obtained by partial differentiation
of the forces and moments with respect to each of the ten independent
variables α, β, p, q, r, $\dot{\alpha}$, $\dot{\beta}$, $\dot{p}$, $\dot{q}$, $\dot{r}$ and second derivatives will be
included; that is, there will be derivatives of the types

$$C_{Y_p} = \frac{\partial C_Y}{\partial\left(\dfrac{p l_r}{U_0}\right)} \quad \text{and} \quad C_{Y_{\alpha p}} = \frac{\partial^2 C_Y}{\partial\alpha \, \partial\left(\dfrac{p l_r}{U_0}\right)}$$

where all derivatives are evaluated at $\alpha = \beta = p = q = r = \dot{\alpha} = \dot{\beta} = \dot{p} =$
$\dot{q} = \dot{r} = 0$. The reason for this choice (which is not customary) will
become more evident later, but it can be seen at once that all deriva-
tives defined in this manner are constant for a given configuration and
that there will be "cross derivatives" of the type $C_{m_{qp}}$ which will
show the mutual influence of the longitudinal and lateral motions. Thus
the total rolling moment due to sideslip, for instance, will be express-
ible as

$$C_{l_\beta}{}^* = C_{l_\beta} + \alpha C_{l_{\alpha\beta}} + \beta C_{l_{\beta\beta}} + p C_{l_{\beta p}} + \ldots$$

For the sake of consistency, all coefficients and derivatives are based on the same reference area S_r and reference length l_r.

If equations (45) and (47) are rewritten with the aid of equations (54) to (56), the necessary partial differentiations can be effected with no difficulty and all the derivatives of the side force, lift, yawing moment, and pitching moment are obtained. The derivation of the rolling-moment derivatives is not quite so straightforward as the others since the expression of equation (51) for the rolling moment contains integrals of the type $\mathbf{R} \oint \varphi \zeta \overline{d\zeta}$ which cannot be handled directly by residues, as mentioned previously. However, when this integral is differentiated with respect to any motion except p or $\dot{p}$, the resulting integral can be related to one of the integrals already evaluated by residues. In particular, if we write once more

$$\varphi = V\varphi_2 + W\varphi_3 + p\varphi_4 + \varphi'$$

it follows from the boundary condition of equation (30) that

$$\frac{\partial \varphi_4}{\partial n} = y \frac{dy}{ds} + z \frac{dz}{ds}$$

or

$$\mathbf{R}(\zeta \overline{d\zeta}) = y\, dy + z\, dz = \frac{\partial \varphi_4}{\partial n}\, ds$$

Thus the integral appearing in C_{l_β}, for example, will be

$$\mathbf{R} \oint \frac{\partial \varphi}{\partial \beta} \zeta \overline{d\zeta} = U_0 \oint \varphi_2 \frac{\partial \varphi_4}{\partial n}\, ds$$

But, by virtue of Green's Theorem (see ref. 13, p. 46),

$$\oint \varphi_2 \frac{\partial \varphi_4}{\partial n}\, ds = \oint \varphi_4 \frac{\partial \varphi_2}{\partial n}\, ds$$

and again from equation (30) it can be seen that

$$\frac{\partial \varphi_2}{\partial n} = \frac{dz}{ds}$$

so that, finally, one can write

$$\mathbf{R} \oint \frac{\partial \varphi}{\partial \beta} \zeta \, \overline{d\zeta} = U_0 \oint \varphi_4 dz = - U_0 \mathbf{I} \oint \frac{\partial \varphi}{\partial p} \overline{d\zeta}$$

This latter integral has already been evaluated with equations (34) and (42) to calculate C_{Y_p}. Similarly, the integrals appearing in the other rolling-moment derivatives can also be evaluated and expressed in terms of the mapping function of the cross section. The actual differentiations to obtain the rolling-moment derivatives are simple enough if one notes that the order of differentiation of the potential φ is important in that the expression of equation (51) has been written for a specific instant of time $(t = 0)$. That is, φ must be differentiated with respect to time first, then integrated to give the rolling moment, and finally differentiated with respect to the desired motion. Thus, since φ is linear in the angles α and β as well as in the angular velocities p, q, and r, one observes that

$$\frac{\partial^2 \varphi}{\partial \alpha \partial t} = \frac{\partial^2 \varphi}{\partial \beta \partial t} = \frac{\partial^2 \varphi}{\partial p \partial t} = \frac{\partial^2 \varphi}{\partial \alpha \partial p} = \ldots = 0$$

and further that

$$\frac{\partial^2 \varphi}{\partial \dot{\alpha} \partial t} = \frac{\partial \varphi}{\partial \alpha}; \qquad \frac{\partial^2 \varphi}{\partial \dot{p} \partial t} = \frac{\partial \varphi}{\partial p}; \qquad \text{etc.}$$

The resulting expressions for the stability derivatives are given in table I, which is arranged so that all the side-force derivatives appear in the first column, all the lift derivatives in the second, and so on. It is found that a number of derivatives vanish identically, that is, regardless of the shape of the cross section. As a matter of fact, all but 84 of the possible 325 first and second derivatives vanish identically. For obvious reasons, the stability derivatives that are identically zero are not listed, but a definite pattern can be seen in table I which shows, for instance, that all second derivatives of C_L, C_Y, C_m, and C_n vanish except those involving p and that there are no second derivatives involving $\dot{\alpha}$, $\dot{\beta}$, $\dot{p}$, $\dot{q}$, or $\dot{r}$. It should be noted that the order of differentiation is immaterial so that $C_{L_{\alpha p}} = C_{L_{p\alpha}}$, etc.

(If this were not the case, the total number of possible derivatives would be 550.) In the next section, a total of 49 relationships are found among the stability derivatives, so that, at most, only 35 derivatives need be calculated directly for any given configuration. It is important to note that the mapping function must be expanded in exactly the form of equation (46) before the proper coefficients can be obtained for use in the formulas of table I. In particular, the coefficient of the σ term must be unity.

Relationships Among the Stability Derivatives

From the general results shown in table I, a number of interesting reciprocal relationships which are independent of the configuration are observed at once. For instance, the side force due to angle of attack is equal to minus the lift due to angle of sideslip ($C_{Y_\alpha} = - C_{L_\beta}$).

Similar equalities among the various derivatives are found throughout and are listed in table II. It should be noted at this point that many of the relationships of table II would be obscured by evaluating the derivatives at $\alpha \neq 0$, as is customarily done.

Beyond these simple equalities, there are some interesting relationships which can be brought out by an integration by parts. For example (see table I),

$$C_{m_\alpha} = - \frac{2}{S_r l_r} \int_0^l (x - c_1) \frac{\partial}{\partial x} [2\pi \mathbf{R}(\bar{a}_1 + r_0{}^2) - S]\, dx$$

$$= - \frac{2}{S_r l_r} \left\{ (l - c_1)[2\pi \mathbf{R}(\bar{a}_1 + r_0{}^2) - S]_{x=l} - \int_0^l [2\pi \mathbf{R}(\bar{a}_1 + r_0{}^2) - S]\, dx \right\}$$

$$= - C_{L_q} + C_{L_{\dot\alpha}}$$

But from table I it is seen that

$$C_{L_q} = \left(\frac{l - c_1}{l_r} \right) C_{L_\alpha}$$

Thus, one finds that

$$C_{L_{\dot\alpha}} = C_{m_\alpha} + \left(\frac{l - c_1}{l_r} \right) C_{L_\alpha}$$

This is a particularly interesting relationship in that it enables one
to calculate from the static lift- and moment-curve slopes a quantity
which would require dynamic tests in the wind tunnel for a direct exper-
imental measurement. Another quantity of interest in this category can
be obtained by integrating by parts the expression for C_{m_q} given in
table I. The resulting relation is

$$C_{m_q} + C_{m_{\dot{\alpha}}} = - \left(\frac{l - c_1}{l_r} \right)^2 C_{L_{\alpha}} \qquad (58)$$

which states that the damping in pitch is proportional to the lift-curve
slope. This result, which is independent of configuration or choice of
axes, was obtained previously by Bryson (ref. 12) whose analysis was
implicitly restricted to bodies having a straight-line axis (i.e., no
camber of the body or the wings). The apparent mass concept, which was
the basis for the analysis of reference 12, will be discussed in a later
section. Other relations obtained here in a manner similar to that for
equations (57) and (58) are given in table II.

It is of some interest to look into
the damping in pitch of wing-body combi-
nations on the basis of equation (58).
Since the lift-curve slope is determined
entirely by the trailing-edge configura-
tion (see table I), it is evident that a
wide variety of airplanes can be treated
at once quite simply. If one considers,
for instance, a configuration whose
trailing-edge cross section consists of
a circle with symmetrically placed
straight lines, as shown in the sketch,
it is known from the transformation (refs.
4 and 12) that the lift-curve slope is
proportional to the quantity

$$\left(1 - \frac{a_0^2}{s_0^2} + \frac{a_0^4}{s_0^4} \right).$$

Thus, from equation (58), it follows that the ratio of the damping in
pitch of the wing-body combination to that of the horizontal wing alone
is also given by this quantity. It is important to note that any changes
in shape ahead of the trailing edge (e.g., camber and thickness of the
wings, variation in fuselage shape, etc.) are immaterial. Thus, for such
configurations, the damping in pitch is plotted in figure 1 and it can
be seen that (1) the body is always destabilizing, and that (2) this
effect is a maximum for a body diameter to wing span ratio of $1/\sqrt{2}$.
The damping in pitch is made a maximum, on the other hand, by bringing
the body to a point (or a line) at or ahead of the wing trailing edge.
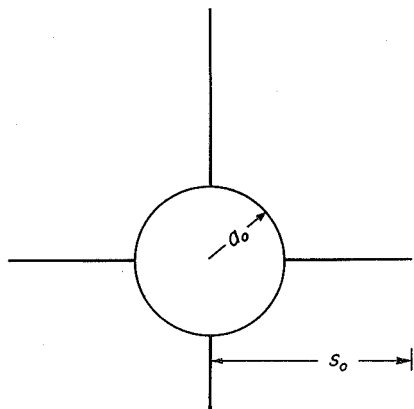
The relationships given in table II are all independent of the configuration, at least to the order of the present analysis. It can be seen from table I that for configurations involving any symmetries (for example if $S\zeta_c = 0$), there will be additional relationships among the stability derivatives. Such a case will be considered in the section titled "Applications of the Theory."

APPARENT MASS

Perhaps the most striking feature of the results presented in table I is the frequent appearance of the quantities $[2\pi \mathbf{R}(\overline{a}_1 - r_0^2) + S]$, $[2\pi \mathbf{R}(\overline{a}_1 + r_0^2) - S]$, and $2\pi \mathbf{I}(\overline{a}_1)$. In fact, since both r_0^2 and S are real, the first two quantities are simply the real parts of $[2\pi(\overline{a}_1 - r_0^2) + S]$ and $[2\pi(\overline{a}_1 + r_0^2) - S]$, respectively, while the third can be written as the imaginary part of either of these bracketed quantities. It now becomes evident that a large number of the stability derivatives depend only on these two bracketed quantities which, in turn, depend only on the shape and size of the airplane cross section. As a matter of fact, it can be shown (ref. 17) that the quantities $\rho \mathbf{R}[2\pi(\overline{a}_1 - r_0^2) + S]$ and $\rho \mathbf{R}[2\pi(\overline{a}_1 + r_0^2) - S]$ are identical with the integrals defined in incompressible flow theory as the additional apparent mass of the cross section in the y and z directions, respectively.

These are given by $\oint \rho \varphi_2 dz$ and $\oint \rho \varphi_3 dy$ (refs. 13 and 17) where φ_2 and φ_3 are the velocity potentials for unit velocity of the cross section in the y and z directions.

The mathematical basis for the use of the apparent mass to calculate the transverse force derivatives of slender bodies in steady flow (as done by Munk and Jones in refs. 1 and 2) was established with Ward's formulation (ref. 5) of the general expression

$$Y - iL = i\rho U_0 \oint_{x=l} \varphi \, d\overline{\zeta} \qquad (59)$$

since a differentiation with respect to angle of attack, for example, yields

$$\frac{\partial(Y - iL)}{\partial \alpha} = i\rho U_0 \oint_{x=l} \frac{\partial \varphi}{\partial \alpha} \, d\overline{\zeta} = -i\rho U_0^2 \oint_{x=l} \varphi_3 d\overline{\zeta}$$

Hence, taking the imaginary part of both sides, one finds

$$L_\alpha = \rho U_0^2 \oint_{x=l} \varphi_3 dy = U_0^2 (m_{33})_{x=l} \tag{60}$$

where m_{33} is the additional apparent mass of the cross section in the z direction for pure translation in the z direction. It thus becomes clear that the lift-curve slope is, in all cases, given by the apparent mass m_{33} evaluated at the base of the body. If equation (59) were differentiated with respect to angle of sideslip rather than angle of attack, then the derivative L_β would be found to involve m_{32} rather than m_{33}, where m_{32} is the apparent mass in the z direction for pure translation in the y direction.

There remains now the question of the relation between the apparent masses and the total forces given by equation (59); that is, under what conditions can the total forces be calculated from the apparent masses? This can perhaps best be clarified by setting

$$\varphi = V_c \varphi_2 + W_c \varphi_3 + \varphi'$$

where the first two terms represent rigid-body translations of the cross section in the y and z directions and φ' represents variations in the shape and size of the cross section with x. For the steady case, the velocity components of the centroid of the cross section are given by

$$V_c = U_0 \left(\beta + \frac{dy_c}{dx} \right)$$

and

$$W_c = - U_0 \left(\alpha - \frac{dz_c}{dx} \right)$$

so that equation (59) can be written in the form

$$Y - iL = iU_0^2 \left[\left(\beta + \frac{dy_c}{dx} \right)(m_{32} - im_{22}) - \left(\alpha - \frac{dz_c}{dx} \right)(m_{33} - im_{23}) \right]_{x=l} +$$

$$i\rho U_0 \oint_{x=l} \varphi' d\bar{\zeta}$$

Note that the quantities $\left(\beta + \dfrac{dy_c}{dx} \right)$ and $\left(\alpha - \dfrac{dz_c}{dx} \right)$ represent the angles

that the line of centroids of the cross sections makes with the flight direction (i.e., the local angles of attack and sideslip). It can now be seen that the complex force of equation (59) is given by the apparent masses and the angles of attack and sideslip of the base cross section,

provided that $\oint_{x=l} \varphi' d\bar{\zeta} = 0.$

As an example, consider first a cambered body with no wings whose cross sections near the base are all circular. In this case

$$\varphi'_{x=l} = k \ ln\sqrt{(y - y_c)^2 + (z - z_c)^2} \quad \text{so that} \quad \oint_{x=l} \varphi' d\overline{\zeta} = 0 \quad \text{and the}$$

apparent mass gives the side force and lift as well as their derivatives. On the other hand, consider a flat plate having deflected partial-span flaps. Here (when the plate is alined with the flight direction), the entire potential at the trailing edge is given by $\varphi'_{x=l}$ whose integral

$\oint_{x=l} \varphi' d\overline{\zeta}$ does not vanish. Hence, in this case, the lift-curve slope is

given by the apparent mass but the lift is not. This is also true for a body of revolution having flat-plate wings at incidence to the body.

For the unsteady case, as a result of a recently published report by Miles (ref. 11), one can show that the stability derivatives can also be obtained from apparent mass considerations. This is most easily seen from the general expression of reference 11

$$Y - iL = i\rho U_o \oint_{x=l} \varphi d\overline{\zeta} + i\rho \frac{\partial}{\partial t} \int_0^l dx \oint \varphi d\overline{\zeta} \tag{61}$$

since, for example,

$$\frac{\partial (Y - iL)}{\partial \left(\frac{\dot{\alpha} l_r}{U_o}\right)} = i\rho \ \frac{\partial}{\partial \left(\frac{\dot{\alpha} l_r}{U_o}\right)} \left(\dot{\alpha} \frac{\partial}{\partial \alpha} \int_0^l dx \oint \varphi d\overline{\zeta}\right) = - \frac{i\rho U_o^2}{l_r} \int_0^l dx \oint \varphi_3 d\overline{\zeta}$$

so that the imaginary part yields

$$L_{\dot{\alpha}} = \frac{U_o^2}{l_r} \int_0^l m_{33} dx \tag{62}$$

It should be noted here again that the total forces themselves are not, in general, given by the apparent masses. Miles also shows in reference 11 that the rolling moment about the wind axis is given by

$$L' = \frac{1}{2} \rho U_o \mathbf{R} \oint_{x=l} Fd(\zeta\overline{\zeta}) + \frac{1}{2} \rho \frac{\partial}{\partial t} \mathbf{R} \int_0^l dx \oint Fd(\zeta\overline{\zeta}) \tag{63}$$

Now, by reasoning exactly parallel to that for the steady case, it can be concluded from equations (12), (61), and (63) that in all cases all of the stability derivatives (except drag) for rigid slender bodies can be obtained from the apparent masses (or, more generally, the "inertia

coefficients"). Also obtainable from the inertia coefficients of the cross sections are (1) the total side force and lift, provided that

$$\oint_{x=l} \varphi' d\bar{\zeta} = 0,$$ (2) the total yawing and pitching moments, provided that

$$\int_0^l (x - c_1)dx \frac{\partial}{\partial x} \oint \varphi' d\bar{\zeta} = 0,$$ and (3) the total rolling moment, provided

that $\mathbf{R} \oint_{x=l} \varphi' \zeta d\bar{\zeta} = 0.$ It is interesting to note that conditions (1) and

(3) involve symmetries of the cross sections only near the base, but that condition (2) is more stringent and is satisfied, for example, by having bilateral symmetry of the cross sections over the entire length of the airplane.

An alternative form for the integrals representing the apparent masses or inertia coefficients can be shown to be identical with the integrals representing the kinetic energy of the fluid associated with any desired unit velocity (linear or angular) of the cross section; for

example, $\oint \rho \varphi_3 dy = - \oint \rho \varphi_3 \frac{\partial \varphi_3}{\partial n} ds.$ However, it is essential to note

that it is only for rigid-body motions of the cross section (as represented, for example, by φ_3) that the two integrals are identical, since

only for such motions does $\frac{\partial \varphi}{\partial n} = - \frac{dy}{ds}$ at the boundary. Thus, it can be

seen that $\oint \rho \varphi' dy \neq - \oint \rho \varphi' \frac{\partial \varphi'}{\partial n} ds$ even if φ' is given proper

dimensions by dividing by a velocity.

Inasmuch as relatively few inertia coefficients have previously been calculated, there seems to be little advantage (other than brevity) in expressing the stability derivatives in terms of these coefficients. It is felt that the formulas of table I involving the mapping function will, in general, be found more useful, although one should certainly make use of any of the coefficients already calculated. In this connection, the reader is referred to a recent paper of Kuerti, McFadden, and Shanks (ref. 17) in which the apparent masses of a number of interesting cross sections are listed for simple translation in the y and z directions.

The apparent mass integral $\oint \varphi_3 dy$ was also calculated for a few

shapes in connection with minimum drag problems in reference 18. However, the integrations there were (for the rectangle) carried over both the exterior and the interior of the cross section since the configuration treated there was indeed a hollow rectangle made up of four thin

wings. It is necessary then, in order to obtain the desired quantity
$[2\pi\mathbf{R}(\overline{a}_1 + r_o{}^2) - S]$, to subtract the cross-sectional area (as pointed
out in ref. 17). It should be pointed out in this regard that all the
results of the present paper are for solid bodies. Thus, if the body con-
tains a jet, one must add to the calculated lift the negative rate of
change of momentum (in the z direction) of the air passing through the
jet. For a simple bent, circular, thin-walled pipe flying approximately
along its axis, a jet exit velocity equal to the flight velocity just
doubles the lift given for the solid circular cross section.

The tabulated values of $\oint \varphi_3 dy$ in reference 18 have been adjusted

for this internal flow and additional values have been calculated here to
extend the range of the variable. The results are plotted in figure 2 to
show the increase in lift-curve slope and damping in pitch obtained by
use of a blunt trailing edge of rectangular cross section, of vertical
end plates near the trailing edge, and of a biplane with sharp trailing
edges. It will be recalled that both the lift-curve slope and the damp-
ing in pitch depend only on the trailing-edge cross section, so the
results of figure 2 are independent of wing thickness, camber, body shape,
etc., ahead of the trailing edge.

It might be mentioned
here that if the apparent
masses of a given cross sec-
tion in two orthogonal
directions are equal, then
the apparent mass of the
cross section is independent
of its direction of trans-
lation. This follows from
the fact that the momentum
vectors and the velocity
vectors add in exactly the
same fashion. In reference
17 it was shown that the
cross sections in the sketch
possess this important property. It also follows, then, that $a_1 = 0$ so
that many of the stability derivatives vanish for such configurations
(see table I).

n fins
n ≥ 3

n corners
regular polygon
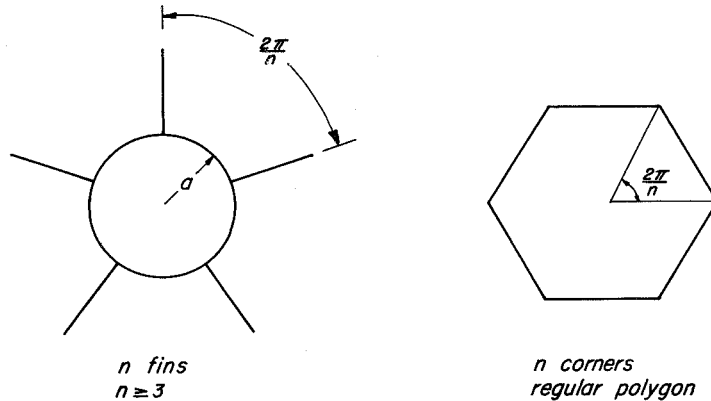
APPLICATIONS OF THE THEORY

In this section, the results of the foregoing analysis will be
applied to the calculation of the stability derivatives for several more
or less special configurations. The first problems to be treated here
will be concerned with the introduction of wing thickness and camber as
parameters since the present analysis is applicable to unsymmetrical

configurations. Then, although the finned body of revolution has been
treated by many authors (e.g., ref. 4, 9, 10, and 12), a plane wing-body
combination will be considered in order to investigate the effect of the
squared terms in the pressure relation. Finally, stability derivatives
will be calculated for a wing-body-vertical-fin combination.

<div align="center">Wings with Thickness and Camber</div>

The quantity "camber," as introduced here, may be complex, the
imaginary part corresponding to the conventional camber in the vertical
(xz) plane and the real part corresponding to a lateral camber or
"wiggles" in the horizontal (xy) plane. Perhaps the simplest configura-
tion of interest for the present problem can be made up of elliptic cross
sections whose eccentricity and position in the lateral planes are arbi-
trary functions of x. The required transformation for such a configura-
tion is (see sketch)
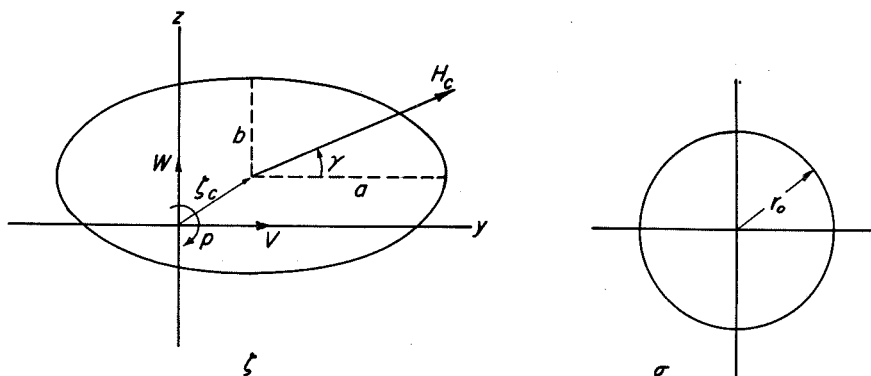
$$\zeta - \zeta_c = \sigma + \frac{a^2 - b^2}{4\sigma} \tag{64}$$

so that

$$a_0 = \zeta_c; \qquad a_1 = \frac{a^2 - b^2}{4}; \qquad a_2 = a_3 = \ldots = 0$$

and the radius of the transformed circle is $r_0 = \frac{a+b}{2}$. These quantities
suffice for the calculation of many of the stability derivatives directly
from table I. However, for the rolling derivatives, the complex potential
is, in general, required. The complex potential in the transformed cir-
cle plane can be derived from reference 16, page 239, and is given by

$$F_1(\sigma) = B \ln \sigma - \frac{H_c(a + b)(b \cos \gamma + ia \sin \gamma)}{2\sigma} +$$

$$\frac{ip(a^2 - b^2)(a + b)^2}{16\sigma^2} + \sum_{n=2}^{\infty} \frac{k_n}{\sigma^n} \qquad (65)$$

where H_c and γ define the lateral velocity of the centroid given by

$$H_c e^{i\gamma} = R + U_o \frac{d\zeta_c}{dx} - ip\zeta_c \qquad (66)$$

The logarithmic term of equation (65) permits a variation in size of the ellipse with x. The series term represents the portion of the potential required to meet the boundary condition of equation (21) when dv/dx is arbitrary (warped body); this permits a variation of the eccentricity b/a with x. If now the potential of equation (65) is transformed to the ζ plane by means of equation (64) and the coefficient of the $1/\zeta$ term is evaluated at $R = p = 0$, it is found that

$$A_{1_o} = -\frac{U_o}{2} \left(a \frac{db}{dx} + b \frac{da}{dx} \right) \zeta_c - U_o \left(\frac{a + b}{2} \right)^2 \frac{d\zeta_c}{dx} + U_o \left(\frac{a^2 - b^2}{4} \right) \frac{d\bar{\zeta}_c}{dx}$$

$$(67)$$

With this result, one can obtain all of the stability derivatives except C_{l_p} and $C_{l_{\dot{p}}}$ directly from the formulas given in tables I and II, for any given configuration in this category. Two examples will now be considered.

The first example will consist of a cambered elliptic cone; that is, an elliptic body with constant eccentricity whose span is a linear function of x. The body axis will be chosen to pass through the center of the base and the camber line will be represented by a sine curve

sec. A-A

sec. B-B
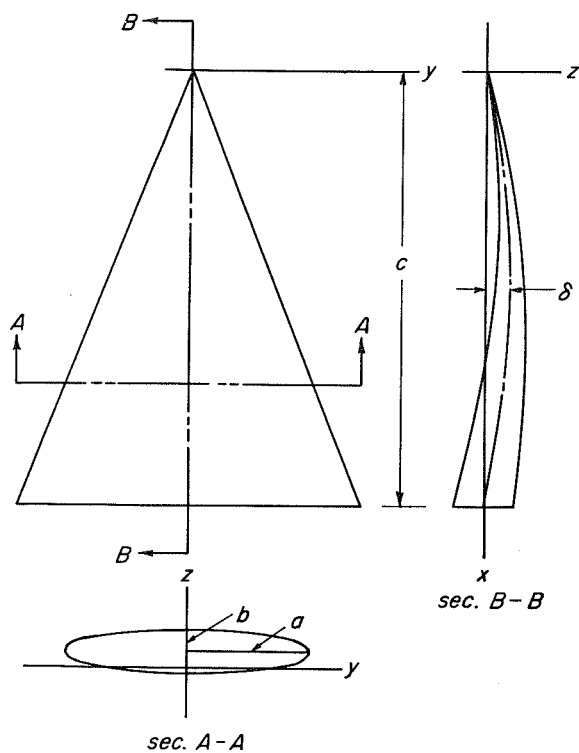
$z_c = \delta \sin \pi x/c$ as shown in the sketch. This body can be thought of as a special case of a cambered triangular wing having a blunt trailing edge. The camber, of course, must be sufficiently small to insure the validity of the slenderness approximations. On the other hand, the thickness ratio as indicated by b/a is arbitrary. Thus the range of b/a from the flat plate ($b/a = 0$) to the circular cone ($b/a = 1$) can be treated as one problem. It should be mentioned that the choice of body axes is arbitrary so that maneuvers about any other set of orthogonal axes fixed in the body could be handled equally well. A few of the interesting stability derivatives have been calculated for this configuration by the formulas of tables I and II and the derivatives C_{n_p} and $C_{n_{\alpha p}}$ are plotted in figure 3. It is seen that C_{n_p} is always negative for positive camber, is linear in the camber, and increases with the thickness. On the other hand, $C_{n_{\alpha p}}$, which is negative in all cases, is independent of the camber and decreases to zero as the thickness ratio increases to one.

As a second example of a configuration having elliptic cross sections, the "wing-like" shape developed by Squire (ref. 19) is chosen. This shape has a variation of eccentricity of the ellipse such that all profile sections (except the midspan section) have a rounded leading edge and a pointed trailing edge. In addition to this particular thickness distribution, for the present problem the wing will be given a camber identical with that taken for the elliptic cone; that is, $z_c = \delta \sin \pi x/c$.

Thus, the wing to be treated here has the shape illustrated in the sketch. For this wing, the major and minor axes of the ellipse are given by

$$a = \frac{A}{4} x \qquad (68)$$

and

$$b = \frac{2t}{c^2} (c - x)x$$

where A is aspect ratio and t is the maximum thickness (thickness of the midspan section at $x = c/2$). Some of the stability derivatives have been calculated for this wing by the formulas of tables I and II and C_{n_p} and $C_{n_{\alpha p}}$ are plotted in figure 4. It is found that C_{n_p} displays, in general, the same variations with camber and thickness as did that for the elliptic cone. However, $C_{n_{\alpha p}}$ displays a trend opposite to that for the elliptic cone. That is, $C_{n_{\alpha p}}$ is seen to increase with thickness, so that the angle-of-attack contribution to the yawing moment due to rolling is apparently heavily influenced by whether the trailing edge is blunt or sharp. The derivative C_{Y_p} was also calculated for both wings and was found to be independent of the thickness. In fact, for either wing, for the axes chosen,

$$C_{Y_p} = - C_{l_\beta} = \frac{2\delta}{c}$$

While this result appears to contradict the corresponding relation found in reference 12 $(C_{Y_p} = C_{l_\beta})$, it simply highlights the fact that the analysis of reference 12 does not include camber although it could be extended to do so. Clearly, if $\delta = 0$ the two results are in agreement. The derivative C_{l_r} was also calculated for both cambered wings and was similarly found to be independent of the thickness. In fact, C_{l_r} was found to have a value equal to C_{n_p} for zero thickness; that is,

$$C_{l_r} = - 0.4508 \; \delta/\text{span}.$$

It is interesting to note that since the trailing-edge cross section of the Squire wing is a straight line, any stability derivatives that depend only on the mapping function of the trailing-edge section (see
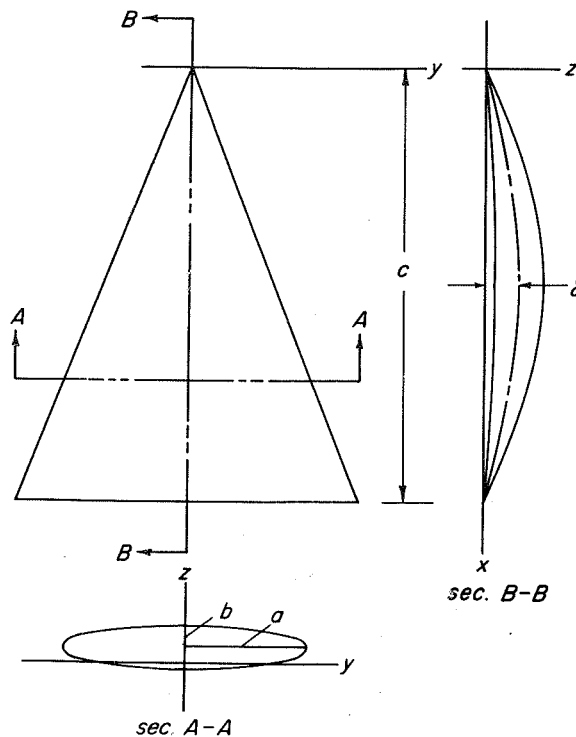
table I) will be the same as for a flat-plate wing (e.g., C_{L_α}, C_{Y_β}, C_{L_β}, C_{L_q}, etc.). It is important also that for an elliptic cross section, the quantity $[2\pi(\bar{a}_1 + r_o^2) - S]$ (apparent mass in the z direction) is independent of the eccentricity, depending only on the semimajor axis a, while the quantity $[2\pi(\bar{a}_1 - r_o^2) + S]$ (apparent mass in the y direction) depends only on b. Thus it can be seen from table I that all of the purely longitudinal derivatives $(C_{L_\alpha}, C_{L_q}, C_{L_{\dot\alpha}}, C_{L_{\dot q}}, C_{m_\alpha}, C_{m_q}, C_{m_{\dot\alpha}}, C_{m_{\dot q}})$ are the same as for a flat-plate wing of local semispan a. Similarly, all of the purely lateral derivatives $(C_{Y_\beta}, C_{n_\beta},$ etc.) are the same as for a flat-plate wing of semispan b if we replace β by minus α, Y by L, and N by M. One can see, therefore, that the ellipse is a very special cross section and tends to obscure some of the effects of thickness. For instance, it was seen in figure 2 that $[2\pi\mathbf{R}(\bar{a}_1 + r_o^2) - S]$ for a rectangle increases with the height of the rectangle and that a blunt trailing edge of rectangular cross section will therefore give an increase in lift-curve slope over a flat plate and a corresponding increase in the damping in pitch.

For the evaluation of rolling moments it would appear from equations (51) and (52) that some of the integrations might be quite difficult because of the nonanalytic character of the integrands. In fact the stability derivatives C_{l_p} and $C_{l_{\dot p}}$ contain the same nonanalytic integrands (see table I). However, the integrations can sometimes be advantageously carried out in the transformed circle plane by the method of residues. For a configuration having an elliptical cross section at the trailing edge, for example, the calculation of the damping in roll C_{l_p} becomes quite simple with this technique. Specifically, from table I,

$$C_{l_p} = \frac{1}{S_r l_r^2} \mathbf{R} \oint_{x=l} \frac{\partial F}{\partial p} d(\zeta\bar\zeta) = \frac{1}{S_r l_r^2} \mathbf{R} \oint_{x=l} \frac{\partial F}{\partial p} \frac{d(\zeta\bar\zeta)}{d\sigma} d\sigma \qquad (69)$$

Now, since equations (64) and (65) for the required transformation and complex potential are already in the form of power series in σ, and since on the circle boundary $\sigma\bar\sigma = r_o^2$, one can immediately write the integrand as a power series in σ and therefore use the method of residues. It is found for this case that the residue of this series is simply $\frac{i}{8}(a_o^2 - b_o^2)^2$ where the subscript refers to the trailing edge. Thus the damping in roll is given by

$$C_{l_p} = \frac{1}{S_r l_r^2}\mathbf{R}\left\{2\pi i\left[\frac{i}{8}(a_o^2 - b_o^2)^2\right]\right\} = -\frac{\pi a_o^4}{4 S_r l_r^2}\left(1 - \frac{b_o^2}{a_o^2}\right)^2 \qquad (70)$$
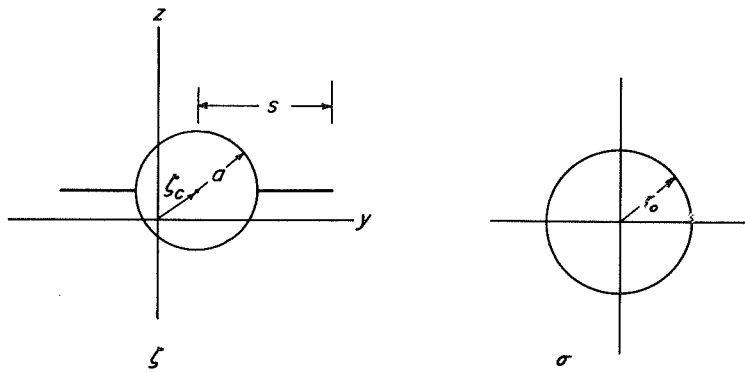
It is seen from equation (70) that for the Squire wing ($b_0 = 0$) the damping in roll is independent of the wing thickness and camber, remaining always at the flat-plate value as given by Ribner (ref. 3). For the elliptic cone, on the other hand, C_{l_p} depends on the thickness and the effect of a blunt trailing edge becomes apparent. Values of C_{l_p} for these cases are plotted in figure 5. It should be noted in general that since $\partial F/\partial p$ is independent of any translational velocity in the cross plane, the damping in roll is not affected by camber.

The device used above to permit the use of the method of residues can always be employed; that is, since $\partial F/\partial p$, ζ, and $\bar{\zeta}$ are all expressible as power series in σ and $\bar{\sigma}$ and since σ and $\bar{\sigma}$ are related by the radius of the transformed circle, the integrand becomes an analytic function of the variable of integration in the transformed plane. However, if the transformation itself is an infinite series (as is the case for the finned body of revolution), then the residue and consequently the damping in roll will emerge as an infinite series involving combinations of all the coefficients of the transformation. This series is, in general, considerably more complicated than that entering into derivatives like C_{Y_p}.

Plane Wing-Body Combination

It will be of some interest to consider here certain aspects of the plane wing-body problem in view of the fact that some stability derivatives had been calculated (see ref. 10) before it was generally realized that the squared terms in the pressure relation must be retained. A number of the simpler derivatives can be obtained quickly from table I if the mapping function of the cross section is known, and one of these will now be compared with the corresponding derivative obtained in reference 10 without the squared terms in the pressure relation. The required mapping function is an infinite series obtained by making two successive Joukowsky transformations (see ref. 4), and it is found that

$$\left.\begin{aligned}
a_0 &= \zeta_c \\[2mm]
a_1 &= \frac{1}{4}\left(s + \frac{a^2}{s}\right)^2 - a^2 \\[2mm]
r_0 &= \frac{1}{2}\left(s + \frac{a^2}{s}\right) \\[2mm]
a_2 &= a_4 = a_6 = \ldots = 0
\end{aligned}\right\} \tag{71}$$

where s is the wing semispan and a is the body radius (see sketch). Hence, many of the stability derivatives vanish by virtue of the fact that a_1 is real (see table I). It is noted that s, a, and ζ_c are here all arbitrary functions of x (within the slenderness approximation) and the body will have a straight axis (plane wing-body) only if ζ_c is a linear function of x. Also, if ζ_c is not a linear function of x then the evaluation of A_{1_0} (which is required for some derivatives) becomes a problem which amounts to determining A_1 of the complex potential for simple translation. This will be done shortly.
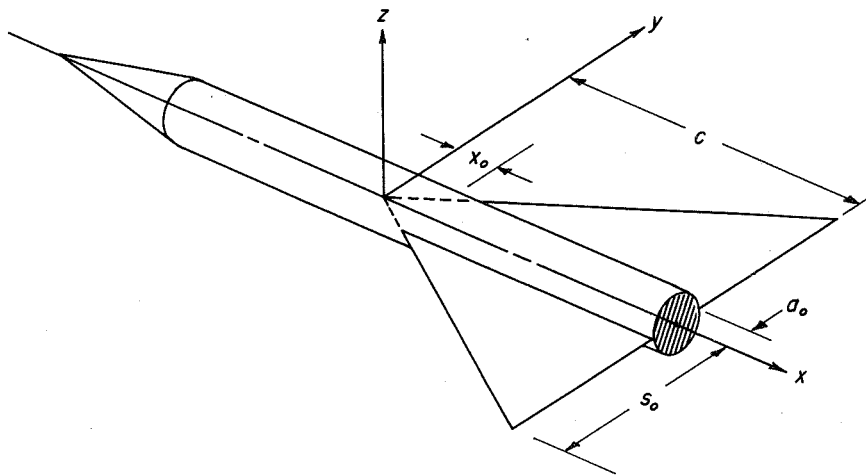
For the purpose of illustrating the influence of the squared terms in the pressure relation, the rolling moment due to sideslip will be calculated for the special case of a flat triangular wing mounted symmetrically on a cone-cylinder as shown in the sketch. For this case, with the axes chosen as shown, it is clear that $\zeta_c = 0$, $a = \text{const.} = a_0$, and $s = s_0(x/c)$. It is further noted that (due to symmetry) there is no rolling moment provided by the portion of the body ahead of $x = x_0$ and that the rolling moment due to sideslip at zero angle of attack is zero ($C_{l_\beta} = 0$). Therefore, the only pertinent derivative[5] to be calculated is $C_{l_{\alpha\beta}}$ which is given by (see table I)

---

[5]For this configuration all of the coupled (second) derivatives of the rolling moment vanish except $C_{l_{\alpha\beta}}$ and $C_{l_{\beta q}}$, and it is assumed here (for purposes of comparison with ref. 10) that $q = 0$.

$$C_{l_{\alpha\beta}} = -\frac{8\pi}{S_r l_r} \int_{x_o}^{c} \left[\frac{1}{4} \left(s + \frac{a^2}{s} \right)^2 - a^2 \right] dx = -\frac{\pi}{3} \left(1 - \frac{a_o}{s_o} \right)^3 \left(1 + 3\frac{a_o}{s_o} \right)$$

$$(72)$$

where S_r and l_r have been taken as the gross wing area and the maximum wing span, respectively. The ratio of this $C_{l_{\alpha\beta}}$ to that for the wing alone ($a_o/s_o = 0$) is plotted in figure 6 and is compared with the corresponding curve of reference 10. It can be seen that the error incurred by the omission of the squared terms in the pressure relation is in excess of 100 percent for ratios of body diameter to wing span greater than 0.5. Now since $C_{Y_{\alpha p}} = -C_{l_{\alpha\beta}}$ according to table II, the side force due to rolling can also be compared with that obtained from a linear pressure relation by means of equation (72). This comparison is presented in figure 7 and it is seen that the difference is even more pronounced than that for the rolling moment due to sideslip. It should be mentioned that if the wing-body combination is cambered, the contribution of rolling moment by the nose will not, in general, vanish, nor will the rolling moment at zero angle of attack.

It has been mentioned that for a general wing-body combination of the cross section discussed above (i.e., ζ_c not a linear function of x), the coefficient of the $1/\zeta$ term in the complex potential must be determined if all of the stability derivatives are to be calculated. The coefficient A_1 for simple translation ($p = 0$) can perhaps most readily be obtained from the complex potential for a flat plate in a uniform stream by use of the transformation
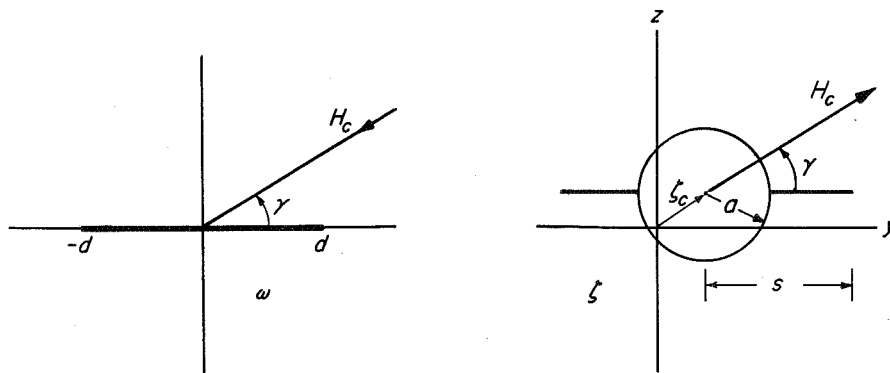
$$\omega = (\zeta - \zeta_c) + \frac{a^2}{\zeta - \zeta_c}$$

(see sketch). The complex potential in the ω plane is given by (see e.g., ref. 16, p. 161)

$$F_1(\omega) = -H_c(\omega \cos\gamma - i\sin\gamma\sqrt{\omega^2 - d^2})$$

$$(73)$$

so that, by using the above transformation and adding a term $H_c \zeta e^{-i\gamma}$ to remove the free stream in the ζ plane and a term $B \ln(\zeta - \zeta_c)$ to allow a variation of the radius a with x, one finds after expansion in series that the coefficient of $1/\zeta$ is (for p = 0)

$$A_1 = - H_c \left[a^2 \cos \gamma - \frac{i}{2} (2a^2 - d^2) \sin \gamma \right] - B \zeta_c \qquad (74)$$

where $d = s + a^2/s$ and it is recalled that $H_c e^{i\gamma} = R + U_0(d\zeta_c/dx)$ for pure translation. Now, by noting that for R = 0

$$\cos \gamma = \frac{U_0}{H_c} \left(\frac{dy_c}{dx} \right)$$

and

$$\sin \gamma = \frac{U_0}{H_c} \left(\frac{dz_c}{dx} \right)$$

one can write finally for this type of configuration

$$A_{1_0} = - U_0 \left[a^2 \frac{dy_c}{dx} - \frac{i}{2} (2a^2 - d^2) \frac{dz_c}{dx} + a \frac{da}{dx} (y_c + iz_c) \right] \qquad (75)$$

With A_{1_0} determined, all of the stability derivatives except C_{l_p} and $C_{l_{\dot{p}}}$ can be obtained directly from tables I and II. The difficulties in determining C_{l_p} and $C_{l_{\dot{p}}}$ have been discussed in the preceding section.

Wing-Body-Vertical-Fin Combination
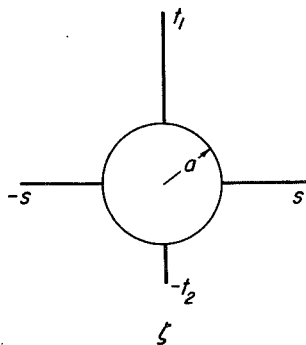
In reference 12, the mapping function was developed for a body of revolution having four flat-plate fins mounted 90° apart (see sketch). Therefore, one can use the formulas of table I directly for such a configuration by first determining the proper coefficients in the expansion of the mapping function. It is important to note that for this purpose, the expansion of the mapping function must be exactly of the form of equation (46). The mapping function given in reference 12 is not of this form (as can be verified by carrying out the

expansion), but it can be modified to give the proper form. The resulting transformation is

$$\left(\zeta - \frac{a^2}{\zeta} \right)^2 - d^2 = \left[\frac{i}{2} (h - f) + \sigma - \frac{(h + f)^2}{16\sigma} \right]^2 \qquad (76)$$
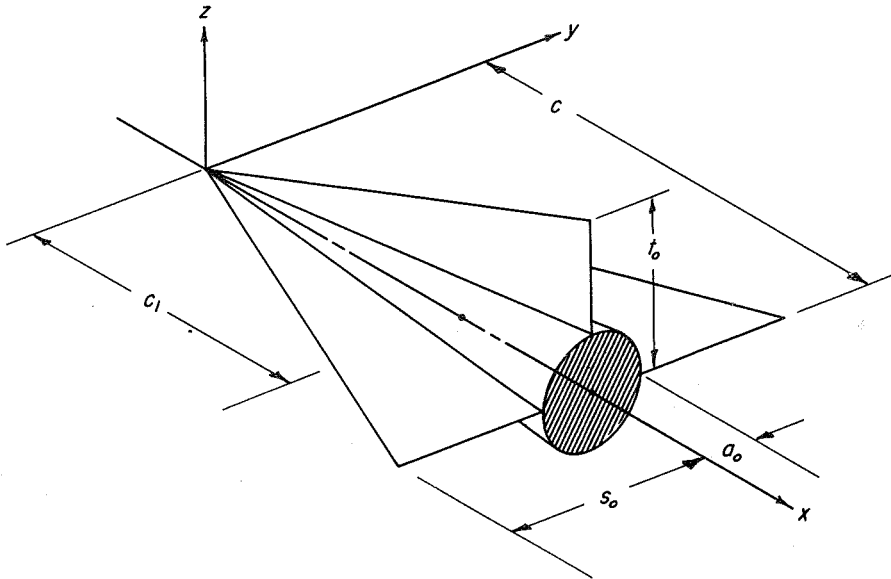
and

$$r_0 = \frac{h + f}{4}$$

where

$$d = s \left(1 - \frac{a^2}{s^2} \right)$$

$$h = \sqrt{ s^2 \left(1 - \frac{a^2}{s^2} \right)^2 + t_1^2 \left(1 + \frac{a^2}{t_1^2} \right)^2 } \; ; \; f = \sqrt{ s^2 \left(1 - \frac{a^2}{s^2} \right)^2 + t_2^2 \left(1 + \frac{a^2}{t_2^2} \right)^2 }$$

and it is found after a somewhat laborious expansion that the first six coefficients are

$$a_0 = \frac{i}{2} (h - f)$$

$$a_1 = a^2 - \left(\frac{h + f}{4} \right)^2 + \frac{d^2}{2}$$

$$a_2 = - \frac{i}{2} (h - f) \left(a^2 + \frac{d^2}{2} \right)$$

$$a_3 = - \left(a^2 + \frac{d^2}{2} \right) \left[\left(\frac{h - f}{2} \right)^2 - \left(\frac{h + f}{4} \right)^2 \right] - \frac{1}{8} (d^2 + 2a^2)^2 - \frac{a^4}{2}$$

$$a_4 = - \frac{i}{2} (h - f) \left\{ \left[2 \left(\frac{h + f}{4} \right)^2 - \left(\frac{h - f}{2} \right)^2 \right] \left(\frac{d^2}{2} + a^2 \right) - \right.$$

$$\left. \frac{3}{8} (d^2 + 2a^2)^2 - \frac{3}{2} a^4 \right\}$$

$$a_5 = \left[\left(\frac{h + f}{4} \right)^4 - 3 \left(\frac{h - f}{2} \right)^2 \left(\frac{h + f}{4} \right)^2 \right] \left(\frac{d^2}{2} + a^2 \right) +$$

$$\left[6 \left(\frac{h - f}{2} \right)^2 - 3 \left(\frac{h + f}{4} \right)^2 \right] \left[\frac{1}{8} (d^2 + 2a^2)^2 + \frac{a^4}{2} \right] +$$

$$\frac{1}{16} (d^2 + 2a^2)^3 + \frac{3}{4} d^2 a^4 + \frac{3}{2} a^6 + \frac{1}{2} \left(\frac{h - f}{2} \right)^4 (d^2 + 2a^2)$$

$$(77)$$

In general, the integrations indicated in table I would have to be performed numerically for a given configuration of the type considered above. However, for a conical configuration, great simplification is achieved and the integrations become trivial. Therefore, a two-parameter conical configuration is chosen to illustrate the effect of a vertical fin on a number of the stability derivatives; that is, the lower fin is removed by setting $t_2 = a$, and t_1 (or t), a, and s are taken to be proportional to x (see sketch). Thus, the coefficients given above and the radius of the transformed circle become proportional to x or x^2 and most of the stability derivatives can be readily calculated. It is noted that for this configuration, with the axes chosen, $A_{1_0} = \zeta_c = 0$. Also, due to the conical property, $C_{n_\beta} = C_{m_\alpha} = 0$ if c_1 is chosen as $2/3$ c.

The stability derivatives obtainable from the coefficient a_1 (which in this case is real) and from the radius of the transformed circle r_0 have been calculated for a range of the parameters a/s and t/s and are plotted in figure 8. The purely longitudinal derivatives are of course unaffected by the vertical fin as seen in figure 8(b) (which is incidentally the same curve as given in figure 1 for a different purpose with regard to a more general configuration).
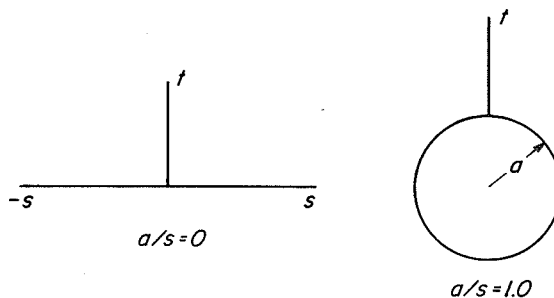
Some interesting and important effects of the vertical fin can be seen in figures 8(a) and 8(c) which show a number of the lateral and "coupled" derivatives. First it should be noted that the two ends of the a/s scale correspond to the extreme configurations shown in the sketch. It is clear that the solid curves of figures 8(a) and 8(c) have no meaning for $a/s > t/s$ since this would correspond to a vertical fin inside the body. Therefore, for values of t/s less than 1, the envelope curves (the dashed curves) corresponding to $a/s = t/s$ have been plotted to fill in

the rest of the range of a/s from 0 to 1. It is seen that even at
a/s = 0 a vertical fin of small span is quite ineffective on both stabil-
ity derivatives I and III (see figs. 8(a) and 8(c)). Hence, the ineffec-
tiveness of small fins is not entirely caused by the body absorbing the
fin, but is partly due to a blanketing effect of the horizontal wing.

The significance of the effect of the vertical fin can perhaps best
be appreciated by considering a relatively familiar derivative $C_{n_{\alpha p}}$
(fig. 8(a)) which can be thought of as the angle-of-attack contribution
to the yawing moment due to rolling. It appears that for fin heights
such that t/s > 1.0 this derivative becomes positive over some portion
of the a/s range (almost the entire range if t/s > 1.5). Thus, for
this configuration, the angle-of-attack contribution to the yawing moment
due to rolling can be changed from adverse (negative) to favorable
(positive) by increasing the height of the vertical fin above about 1.5
times the wing semispan, depending on the body radius.

From the coefficients given in equation (77), it is difficult to
make any statement regarding the convergence of the series required for
derivatives such as C_{n_p} (see table I). Therefore, one is at a loss to
say how many terms of the expansion must be retained for satisfactory
calculations. In order to get some idea of the convergence, the deri-
vatives involving the series were calculated using 2, 3, 4, 5, and 6
terms in the series and the results are presented in figure 9. It appears
that for some cases four terms would be sufficient. The results of fig-
ure 9 indicate a strong blanketing effect of the wing on the vertical fin
for t/s < 1. It can be seen that for a/t = 1 (plane wing-body)
$C_{n_p} = C_{n_{\dot{p}}} = \ldots = 0.$

In reference 20, one of the configurations treated corresponds to
the present conical wing-body-vertical-fin combination for a = 0 (no
body). As this furnishes an interesting check on the present calcula-
tions, the appropriate values of C_{Y_p}, C_{Y_β}, and C_{l_β} have been taken from
that report[6] and are plotted on figures 8 and 9. It can be seen that the
agreement is excellent, even for those derivatives calculated with only
a few terms of the infinite series (fig. 9). It should be noted in fig-
ure 9 that wherever the best approximation curve (representing 6 terms
in the series) cannot be seen, it is because the results were essentially
identical with the previous approximation.

It is interesting to note that for a cruciform wing-body combination
($t_1 = t_2 = s$), according to equations (76) and (77) and succeeding terms,
one finds that $a_0 = a_1 = a_2 = a_4 = a_6 = \ldots = 0$ so that many of the
stability derivatives of table I vanish due to the symmetry of such a
configuration if the axis of symmetry is chosen as the x axis; for
example, here again $C_{n_p} = C_{n_{\dot{p}}} = \ldots = 0.$

---

[6]The values of C_{Y_p}, C_{Y_β}, and C_{l_β} were taken from figures 11, 23,
and 24 of reference 20 since there appear to be some typographical errors
in equation (58) of that report.

CONCLUDING REMARKS

A general analysis has been presented for determining the forces (except drag) and moments and the stability derivatives of a slowly maneuvering slender wing-body combination of arbitrary cross section. The results of the general analysis appear as (1) formulas for the forces and moments in terms of the airplane shape and motions and (2) formulas for the nonzero stability derivatives in terms of the mapping functions of the cross sections.

Stability derivatives of the first and second order have been considered so that the interdependence of the longitudinal and lateral motions is included. A number of relationships among the various stability derivatives were found which are independent of the shape of the airplane, so that, at most, only 35 of a total of 325 first and second derivatives need be calculated directly.

In order to bring out these relationships, the stability derivatives have been defined somewhat differently from the usual derivatives. For example, the usual derivative of rolling moment due to sideslip would, in the present analysis, be given by

$$C_{l_\beta}^* = C_{l_\beta} + \alpha C_{l_{\alpha\beta}} + \beta C_{l_{\beta\beta}} + p C_{l_{\beta p}} + q C_{l_{\beta q}} + r C_{l_{\beta r}}$$

All derivatives as defined in this paper, then, are constant for a given airplane. Time rates of change of the angles and angular velocities have also been included, although these effects vanish for the particular derivative above.

The use of the apparent mass concept for problems in slender-body theory has been discussed in the light of the present analysis and on the basis of previous treatments of slender-body problems by momentum methods. It is demonstrated that all of the stability derivatives can be calculated from the apparent masses (or inertia coefficients), but that the general expressions for the total forces and moments involve additional terms.

From the results of the general analysis, some of the stability derivatives have been calculated for (1) two triangular wings having thickness and camber, (2) a plane wing-body combination, and (3) a wing-body-vertical-fin combination. These three cases have been used to show, respectively, (1) the effects of camber, thickness, and blunt trailing edge, (2) the influence of the squared terms in the pressure relation, and, (3) the effect of a vertical fin on the various stability derivatives.

It was found that the effect of thickness on the angle-of-attack contribution to the yawing moment due to rolling was essentially opposite for blunt and sharp trailing edges, but the effect at zero angle of attack was similar in both cases. In both cases, the angle-of-attack

contribution was independent of the camber while the zero-angle-of-attack contribution was linear in the camber.

The damping in pitch was shown to be proportional to the lift-curve slope and therefore to depend only on the base cross section. On this basis, the lift-curve slopes and damping in pitch were calculated for (1) a wing-body-vertical-fin combination, (2) a blunt trailing edge of rectangular cross section, (3) a sharp trailing edge with end plates, and (4) a biplane with sharp trailing edges. Sizable increases over the flat-plate values are shown in the last three cases.

The derivatives usually called C_{Y_p} and C_{l_β} were calculated to be more than 100 percent in error if the squared terms in the pressure relation are neglected in the case of a plane wing-body combination of body diameter to wing span ratio of 0.5 or greater.

A number of stability derivatives were calculated for a conical wing-body-vertical-tail combination and the variations with body diameter to wing span ratio were plotted for various vertical tail spans. The influence of the vertical fin was found to be markedly altered by the blanketing effect of the wing for small vertical tail spans.

Ames Aeronautical Laboratory
    National Advisory Committee for Aeronautics
        Moffett Field, Calif., June 10, 1954

APPENDIX A

DIFFERENTIATION OF A CONTOUR INTEGRAL
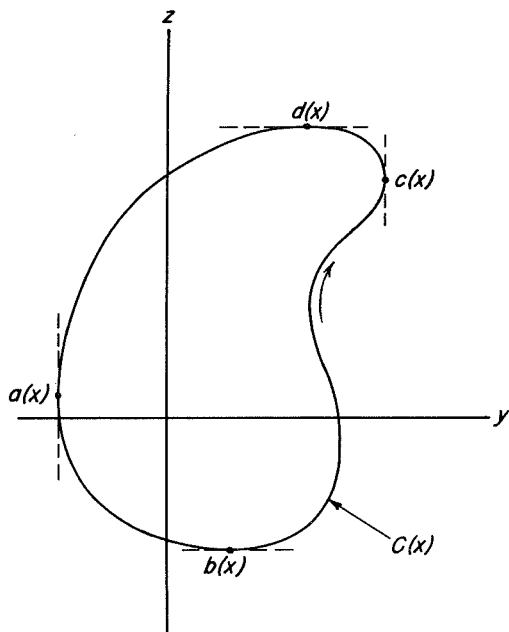
Consider a differentiation of the contour integral $\oint \varphi \, d\bar{\zeta}$ with respect to x, where the contour is a smooth closed path that depends on x, as shown in the sketch. The four points on the curve, designated a, b, c, and d, represent the maximum positive and negative values of y and z, so that the function φ on the contour between a and c can be designated φ_{lower} (or simply φ_l), that between c and a, φ_{upper} (or φ_u), and those between b and d and between d and b, φ_+ and φ_-, respectively. Thus one can write

$$\frac{\partial}{\partial x} \oint \varphi \, d\bar{\zeta} = \frac{\partial}{\partial x} \int_C \varphi \, dy - i \frac{\partial}{\partial x} \int_C \varphi \, dz = \frac{\partial}{\partial x} \int_{a(x)}^{c(x)} \varphi_l \, dy +$$

$$\frac{\partial}{\partial x} \int_{c(x)}^{a(x)} \varphi_u \, dy - i \frac{\partial}{\partial x} \int_{b(x)}^{d(x)} \varphi_+ \, dz - i \frac{\partial}{\partial x} \int_{d(x)}^{b(x)} \varphi_- \, dz$$

so that there are now four line integrals to be differentiated. This can be done directly by means of the formula

$$\frac{\partial}{\partial x} \int_{r(x)}^{s(x)} f(x,y) \, dy = \int_{r(x)}^{s(x)} \frac{\partial f}{\partial x} \, dy + \frac{\partial s}{\partial x} f(s,x) - \frac{\partial r}{\partial x} f(r,x)$$

which gives

$$\frac{\partial}{\partial x} \oint \varphi d\bar{\zeta} = \int_{a(x)}^{c(x)} \frac{\partial \varphi_l[x,y,Z_1(x,y)]}{\partial x} \, dy + \frac{\partial c}{\partial x} \varphi_l(c,x) - \frac{\partial a}{\partial x} \varphi_l(a,x) +$$

$$\int_{c(x)}^{a(x)} \frac{\partial \varphi_u[x,y,Z_1(x,y)]}{\partial x} \, dy + \frac{\partial a}{\partial x} \varphi_u(a,x) - \frac{\partial c}{\partial x} \varphi_u(c,x) -$$

$$i\left\{ \int_{b(x)}^{d(x)} \frac{\partial \varphi_+[x,z,Y_1(x,z)]}{\partial x} \, dz + \frac{\partial d}{\partial x} \varphi_+(d,x) - \frac{\partial b}{\partial x} \varphi_+(b,x) \right\} -$$

$$i\left\{ \int_{d(x)}^{b(x)} \frac{\partial \varphi_-[x,z,Y_1(x,z)]}{\partial x} \, dz + \frac{\partial b}{\partial x} \varphi_-(b,x) - \frac{\partial d}{\partial x} \varphi_-(d,x) \right\}$$

where $z = Z_1(x,y)$ and $y = Y_1(x,z)$ are alternative expressions for the contour C and must be single-valued between the prescribed limits of integration.

Now, if the velocity potential φ is single-valued on the contour, then

$$\varphi_u = \varphi_l \quad \text{at} \quad a(x) \text{ and } c(x)$$

and

$$\varphi_+ = \varphi_- \quad \text{at} \quad b(x) \text{ and } d(x)$$

so that all four of the additional terms above cancel and one finds, after combining like integrals, that

$$\frac{\partial}{\partial x} \oint \varphi d\bar{\zeta} = \int_C \frac{\partial \varphi[x,y,Z_1(x,y)]}{\partial x} \, dy - i \int_C \frac{\partial \varphi[x,z,Y_1(x,z)]}{\partial x} \, dz$$

But the partial derivatives can be rewritten in the form

$$\frac{\partial \varphi[x,y,Z_1(x,y)]}{\partial x} = \left[\frac{\partial \varphi}{\partial x} + \frac{\partial \varphi}{\partial z} \frac{\partial Z_1}{\partial x} \right]_{z=Z_1(x,y)}$$

and

$$\frac{\partial \varphi[x,z,Y_1(x,z)]}{\partial x} = \left[\frac{\partial \varphi}{\partial x} + \frac{\partial \varphi}{\partial y} \frac{\partial Y_1}{\partial x} \right]_{y=Y_1(x,z)}$$

Therefore, since $\dfrac{\partial \varphi}{\partial x}\bigg]_{z=Z_1} = \dfrac{\partial \varphi}{\partial x}\bigg]_{y=Y_1}$, the final result is

$$\frac{\partial}{\partial x} \oint \varphi\, d\bar{\zeta} = \int_C \frac{\partial \varphi}{\partial x}\, dy + \int_C \frac{\partial \varphi}{\partial z} \frac{\partial Z_1}{\partial x}\, dy - i \int_C \frac{\partial \varphi}{\partial x}\, dz - i \int_C \frac{\partial \varphi}{\partial y} \frac{\partial Y_1}{\partial x}\, dz$$

$$= \oint \frac{\partial \varphi}{\partial x}\, d\bar{\zeta} + \int_C \frac{\partial \varphi}{\partial z} \frac{\partial Z_1}{\partial x}\, dy - i \int_C \frac{\partial \varphi}{\partial y} \frac{\partial Y_1}{\partial x}\, dz$$

APPENDIX B

THE RESIDUE A_1 OF THE COMPLEX POTENTIAL

From equation (31) it follows that

$$2i\psi_s = \overline{R}\zeta - R\overline{\zeta} + ip\zeta\overline{\zeta} + 2iU_0 \int \frac{d\nu}{dx}\,ds + 2iG(x,t)$$

Now, if one maps the body contour in the ζ plane onto a circle of radius r_0, center the origin, in the σ plane by the transformation

$$\zeta = f(\sigma) = \sigma + \sum_{n=0}^{\infty} \frac{a_n}{\sigma^n}$$

(where a_n is in general complex) then the "boundary function" of Milne-Thomson (ref. 16, p. 237) is obtained. Noting that on the circle boundary $\sigma\overline{\sigma} = r_0^2$ so that

$$\overline{\zeta} = \overline{f}(\overline{\sigma}) = \frac{r_0^2}{\sigma} + \sum_{n=0}^{\infty} \frac{\overline{a}_n}{r_0^{2n}}\,\sigma^n$$

one can write the boundary function as

$$2i\psi_s = \overline{R}\left(\sigma + \sum_{n=0}^{\infty} \frac{a_n}{\sigma^n}\right) - R\left(\frac{r_0^2}{\sigma} + \sum_{n=0}^{\infty} \frac{\overline{a}_n}{r_0^{2n}}\,\sigma^n\right) +$$

$$ip\left(\sigma + \sum_{n=0}^{\infty} \frac{a_n}{\sigma^n}\right)\left(\frac{r_0^2}{\sigma} + \sum_{n=0}^{\infty} \frac{\overline{a}_n}{r_0^{2n}}\,\sigma^n\right) + T(\sigma) + 2iG(x,t)$$

where $T(\sigma)$ is simply $2iU_0 \int \frac{d\nu}{dx}\,ds$ expressed as a function of σ.

It has been demonstrated in reference 16 that this boundary function can be satisfied by setting the complex potential equal to the part of $2i\psi_s$ containing only the negative powers of σ. Thus one can set

$$F = \overline{R}\sum_{n=1}^{\infty} \frac{a_n}{\sigma^n} - R\frac{r_0^2}{\sigma} + ip\frac{r_0^2}{\sigma}\sum_{n=0}^{\infty} \frac{a_n}{\sigma^n} + ip\sum\sum_{m>n} \frac{a_m\overline{a}_n}{r_0^{2n}\sigma^{m-n}} + T_N(\sigma)$$

where $T_N(\sigma)$ represents the portion of T containing negative powers of σ. The residue A_1 of F can then be expressed as

$$A_1 = \bar{R}a_1 - Rr_o^2 + ip\left(a_o r_o^2 + a_1\bar{a}_o + \frac{a_2\bar{a}_1}{r_o^2} + \frac{a_3\bar{a}_2}{r_o^4} + \cdots\right) + A_{1_o}$$

where A_{1_o} is the residue of $T_N(\sigma)$ and it is noted that A_{1_o} can depend only on the shape of the cross section and not on any of the airplane motions; that is, A_{1_o} must be a function of x alone and is simply the value of A_1 at $R = \bar{R} = p = 0$. Therefore A_{1_o} is zero for any configuration possessing an axis of symmetry if that axis is chosen as the x axis.

It can be seen that A_1 is independent of the rolling velocity p provided that a_o vanishes and that either all the odd n or all the even n are absent in the expansion of $f(\sigma)$. This leads to the considerations of symmetry given in the text. It should be noted that for symmetrical shapes a_o is the centroid of the cross section.

REFERENCES

1. Jones, Robert T.: Properties of Low-Aspect-Ratio Pointed Wings at Speeds Below and Above the Speed of Sound. NACA Rep. 835, 1946. (Formerly NACA TN 1032)

2. Munk, Max M.: The Aerodynamic Forces on Airship Hulls. NACA Rep. 184, 1924.

3. Ribner, Herbert S.: The Stability Derivatives of Low-Aspect-Ratio Triangular Wings at Subsonic and Supersonic Speeds. NACA TN 1423, 1947.

4. Spreiter, John R.: Aerodynamic Properties of Slender Wing-Body Combinations at Subsonic, Transonic, and Supersonic Speeds. NACA TN 1662, 1948.

5. Ward, G. N.: Supersonic Flow Past Slender Pointed Bodies. Quart. Jour. Mech. and Appl. Math., vol. 2, pt. 1, 1949, pp. 75-98.

6. Adams, Mac C., and Sears, W. R.: Slender-Body Theory - Review and Extension. Jour. Aero. Sci., vol. 20, no. 2, Feb. 1953, pp. 85-98.

7. Heaslet, Max. A., and Lomax, Harvard: The Calculation of Pressure on Slender Airplanes in Subsonic and Supersonic Flow. NACA TN 2900, 1953.

8. Phythian, J. E.: Some Unsteady Motions of a Slender Body Through an Inviscid Gas. Quart. Jour. Mech. and Appl. Math., vol. 5, pt. 3, Sept. 1952, pp. 301-317.

9. Lomax, Harvard, and Heaslet, Max. A.: Damping-in-Roll Calculations for Slender Swept-Back Wings and Slender Wing-Body Combinations. NACA TN 1950, 1949.

10. Nonweiler, T.: Theoretical Stability Derivatives of a Highly Swept Delta Wing and Slender Body Combination. College of Aeronautics, Cranfield. Rep. 50, 1951.

11. Miles, John W.: Unsteady Supersonic Flow Past Slender Pointed Bodies. Naval Ordnance Test Station, Inyokern, NAVORD Rep. 2031, 1953.

12. Bryson, Arthur E.: Stability Derivatives for a Slender Missile With Application to a Wing-Body-Vertical-Tail Configuration. Jour. Aero. Sci., vol. 20, no. 5, May 1953, pp. 297-308.

13. Lamb, Horace: Hydrodynamics. Sixth edition, Dover Pub., New York, 1945.

14. Duncan, W. J.: The Principles of the Control and Stability of Air-
     craft. Cambridge University Press (England), 1952.

15. Blasius, H.: Funktiontheoretische Methoden in der Hydrodynamik.
     Zeitschr. für Math. und Phys. 58, 1910.

16. Milne‑Thomson, L. M.: Theoretical Hydrodynamics. Second edition,
     MacMillan and Co., Ltd., N. Y., 1950.

17. Kuerti, G., McFadden, J. A., and Shanks, D.: Virtual Mass of
     Cylinders With Radial Fins and of Polygonal Prisms. Naval
     Ordnance Laboratory, White Oak, Maryland. NAVORD Rep. 2295,
     1952.

18. von Kármán, Th., and Burgers, J. M.: General Aerodynamic Theory -
     Perfect Fluids. Vol. II of Aerodynamic Theory, Div. E, ch. 4,
     W. F. Durand, ed., Julius Springer (Berlin), 1935, pp. 203-214.

19. Squire, H. B.: An Example in Wing Theory at Supersonic Speed.
     R. & M. No. 2549, British ARC, 1947.

20. Bobbitt, Percy J., and Malvestuto, Frank S., Jr.: Estimation of
     Forces and Moments due to Rolling for Several Slender-Tail Con-
     figurations at Supersonic Speeds. NACA TN 2955, 1953.

TABLE I.- STABILITY DERIVATIVES

$$C_{Y_\alpha} = \frac{4\pi}{S_r}\mathbf{I}(\bar{a}_1)_{x=l}$$

$$C_{Y_\beta} = \frac{2}{S_r}\left[2\pi\mathbf{R}(\bar{a}_1 - r_o^2) + S\right]_{x=l}$$

$$C_{Y_p} = \frac{4}{l_r S_r}\mathbf{I}\left[\pi(\bar{a}_o r_o^2 + \bar{a}_1 a_o + \cdots)_{x=l} - (S\bar{\zeta}_c)_{x=l} - \frac{\pi}{u_o}\int_0^l \bar{A}_{1o}\,dx\right]$$

$$C_{Y_q} = \frac{4\pi}{S_r l_r}(l - c_1)\mathbf{I}(\bar{a}_1)_{x=l}$$

$$C_{Y_r} = -\frac{2(l - c_1)}{S_r l_r}\left[2\pi\mathbf{R}(\bar{a}_1 - r_o^2) + S\right]_{x=l}$$

$$C_{Y_{\dot\alpha}} = \frac{4\pi}{l_r S_r}\mathbf{I}\int_0^l \bar{a}_1\,dx$$

$$C_{Y_{\dot\beta}} = \frac{2}{S_r l_r}\int_0^l\left[2\pi\mathbf{R}(\bar{a}_1 - r_o^2) + S\right]dx$$

$$C_{Y_{\dot p}} = \frac{4\pi}{S_r l_r^2}\mathbf{I}\int_0^l(\bar{a}_o r_o^2 + \bar{a}_1 a_o + \cdots)dx$$

$$C_{Y_{\dot q}} = \frac{4\pi}{S_r l_r^2}\mathbf{I}\int_0^l(x - c_1)\bar{a}_1\,dx$$

$$C_{Y_{\dot r}} = -\frac{2}{S_r l_r^2}\int_0^l(x - c_1)\left[2\pi\mathbf{R}(\bar{a}_1 - r_o^2) + S\right]dx$$

$$C_{Y_{\alpha p}} = \frac{8\pi}{S_r l_r}\mathbf{R}\int_0^l \bar{a}_1\,dx$$

$$C_{Y_{\beta p}} = -\frac{8\pi}{S_r l_r}\mathbf{I}\int_0^l \bar{a}_1\,dx$$

$$C_{Y_{pp}} = \frac{4}{S_r l_r^2}\mathbf{R}\int_0^l\left[2\pi(\bar{a}_o r_o^2 + \bar{a}_1 a_o + \cdots) - S\bar{\zeta}_c\right]dx$$

$$C_{Y_{pq}} = \frac{2}{S_r l_r^2}\int_0^l(x - c_1)\left[2\pi\mathbf{R}(\bar{a}_1 + r_o^2) - S\right]dx$$

$$C_{Y_{pr}} = \frac{4\pi}{S_r l_r^2}\mathbf{I}\int_0^l(x - c_1)\bar{a}_1\,dx$$

$$C_{L_\alpha} = \frac{2}{S_r}\left[2\pi\mathbf{R}(\bar{a}_1 + r_o^2) - S\right]_{x=l}$$

$$C_{L_\beta} = -\frac{4\pi}{S_r}\mathbf{I}(\bar{a}_1)_{x=l}$$

$$C_{L_p} = \frac{4}{l_r S_r}\mathbf{R}\left[\pi(\bar{a}_o r_o^2 + \bar{a}_1 a_o + \cdots)_{x=l} - (S\bar{\zeta}_c)_{x=l} - \frac{\pi}{u_o}\int_0^l \bar{A}_{1o}\,dx\right]$$

$$C_{L_q} = \frac{2(l - c_1)}{S_r l_r}\left[2\pi\mathbf{R}(\bar{a}_1 + r_o^2) - S\right]_{x=l}$$

$$C_{L_r} = \frac{4\pi}{S_r l_r}(l - c_1)\mathbf{I}(\bar{a}_1)_{x=l}$$

$$C_{L_{\dot\alpha}} = -\frac{2}{S_r l_r}\int_0^l\left[2\pi\mathbf{R}(\bar{a}_1 + r_o^2) - S\right]dx$$

$$C_{L_{\dot\beta}} = -\frac{4\pi}{S_r l_r}\mathbf{I}\int_0^l \bar{a}_1\,dx$$

$$C_{L_{\dot p}} = \frac{4\pi}{S_r l_r^2}\mathbf{R}\int_0^l(\bar{a}_o r_o^2 + \bar{a}_1 a_o + \cdots)dx$$

$$C_{L_{\dot q}} = \frac{2}{S_r l_r^2}\int_0^l(x - c_1)\left[2\pi\mathbf{R}(\bar{a}_1 + r_o^2) - S\right]dx$$

$$C_{L_{\dot r}} = \frac{4\pi}{S_r l_r^2}\mathbf{I}\int_0^l(x - c_1)\bar{a}_1\,dx$$

$$C_{L_{\alpha p}} = -\frac{8\pi}{S_r l_r}\mathbf{I}\int_0^l \bar{a}_1\,dx$$

$$C_{L_{\beta p}} = -\frac{8\pi}{S_r l_r}\mathbf{R}\int_0^l \bar{a}_1\,dx$$

$$C_{L_{pp}} = -\frac{4}{S_r l_r^2}\mathbf{I}\int_0^l\left[2\pi(\bar{a}_o r_o^2 + \bar{a}_1 a_o + \cdots) - S\bar{\zeta}_c\right]dx$$

$$C_{L_{pq}} = -\frac{4\pi}{S_r l_r^2}\mathbf{I}\int_0^l(x - c_1)\bar{a}_1\,dx$$

$$C_{L_{pr}} = \frac{2}{S_r l_r^2}\int_0^l(x - c_1)\left[2\pi\mathbf{R}(\bar{a}_1 - r_o^2) + S\right]dx$$

$$C_{n_\alpha} = -\frac{4\pi}{S_r l_r}\mathbf{I}\int_0^l(x - c_1)\frac{\partial\bar{a}_1}{\partial x}\,dx$$

$$C_{n_\beta} = -\frac{2}{S_r l_r}\int_0^l(x - c_1)\frac{\partial}{\partial x}\left[2\pi\mathbf{R}(\bar{a}_1 - r_o^2) + S\right]dx$$

$$C_{n_p} = -\frac{4}{S_r l_r^2}\mathbf{I}\left[\pi\int_0^l(x - c_1)\frac{\partial}{\partial x}(\bar{a}_o r_o^2 + \bar{a}_1 a_o + \cdots)dx - \int_0^l(x - c_1)\frac{\partial}{\partial x}(S\bar{\zeta}_c)dx - \frac{\pi}{u_o}\int_0^l(x - c_1)\bar{A}_{1o}\,dx\right]$$

$$C_{n_q} = -\frac{4\pi}{S_r l_r^2}\mathbf{I}\left[\int_0^l(x - c_1)^2\frac{\partial\bar{a}_1}{\partial x}\,dx + \int_0^l(x - c_1)\bar{a}_1\,dx\right]$$

$$C_{n_r} = \frac{2}{S_r l_r^2}\left\{\int_0^l(x - c_1)^2\frac{\partial}{\partial x}\left[2\pi\mathbf{R}(\bar{a}_1 - r_o^2) + S\right]dx + \int_0^l(x - c_1)\left[2\pi\mathbf{R}(\bar{a}_1 - r_o^2) + S\right]dx\right\}$$

$$C_{n_{\dot\alpha}} = -\frac{4\pi}{S_r l_r^2}\mathbf{I}\int_0^l(x - c_1)\bar{a}_1\,dx$$

$$C_{n_{\dot\beta}} = -\frac{2}{S_r l_r^2}\int_0^l(x - c_1)\left[2\pi\mathbf{R}(\bar{a}_1 - r_o^2) + S\right]dx$$

$$C_{n_{\dot p}} = -\frac{4\pi}{S_r l_r^3}\mathbf{I}\int_0^l(x - c_1)(\bar{a}_o r_o^2 + \bar{a}_1 a_o + \cdots)dx$$

$$C_{n_{\dot q}} = -\frac{4\pi}{S_r l_r^3}\mathbf{I}\int_0^l(x - c_1)^2\bar{a}_1\,dx$$

$$C_{n_{\dot r}} = \frac{2}{S_r l_r^3}\int_0^l(x - c_1)^2\left[2\pi\mathbf{R}(\bar{a}_1 - r_o^2) + S\right]dx$$

$$C_{n_{\alpha p}} = -\frac{8\pi}{S_r l_r^2}\mathbf{R}\int_0^l(x - c_1)\bar{a}_1\,dx$$

$$C_{n_{\beta p}} = \frac{8\pi}{S_r l_r^2}\mathbf{I}\int_0^l(x - c_1)\bar{a}_1\,dx$$

$$C_{n_{pp}} = -\frac{4}{S_r l_r^3}\mathbf{R}\left[2\pi\int_0^l(x - c_1)(\bar{a}_o r_o^2 + \bar{a}_1 a_o + \cdots)dx - \int_0^l(x - c_1)S\bar{\zeta}_c\,dx\right]$$

$$C_{n_{pq}} = -\frac{2}{S_r l_r^3}\int_0^l(x - c_1)^2\left[2\pi\mathbf{R}(\bar{a}_1 + r_o^2) - S\right]dx$$

$$C_{n_{pr}} = -\frac{4\pi}{S_r l_r^3}\mathbf{I}\int_0^l(x - c_1)^2\bar{a}_1\,dx$$

Note: Infinite series indicated is in all cases $\bar{a}_o r_o^2 + \bar{a}_1 a_o + \dfrac{\bar{a}_2 a_1}{r_o^2} + \dfrac{\bar{a}_3 a_2}{r_o^4} + \dfrac{\bar{a}_4 a_3}{r_o^6} + \cdots$

Page intentionally left blank

TABLE I.- STABILITY DERIVATIVES - Concluded

Left column:

$$C_{m_\alpha} = -\frac{2}{S_r l_r} \int_0^l (x - c_1) \frac{\partial}{\partial x} \left[2\pi \mathbf{R}(\bar{a}_1 + r_0^2) - S \right] dx$$

$$C_{m_\beta} = \frac{4\pi}{S_r l_r} \mathbf{I} \int_0^l (x - c_1) \frac{\partial \bar{a}_1}{\partial x} dx$$

$$C_{m_p} = -\frac{4}{S_r l_r^2} \mathbf{R} \left[\pi \int_0^l (x - c_1) \frac{\partial}{\partial x} (\bar{a}_0 r_0^2 + \bar{a}_1 a_0 + \dots) dx - \int_0^l (x - c_1) \frac{\partial}{\partial x} (S \bar{\zeta}_c) dx - \frac{\pi}{u_0} \int_0^l (x - c_1) \bar{A}_{1_0} dx \right]$$

$$C_{m_q} = -\frac{2}{S_r l_r^2} \left\{ \int_0^l (x - c_1)^2 \frac{\partial}{\partial x} \left[2\pi \mathbf{R}(\bar{a}_1 + r_0^2) - S \right] dx + \int_0^l (x - c_1) \left[2\pi \mathbf{R}(\bar{a}_1 + r_0^2) - S \right] dx \right\}$$

$$C_{m_r} = -\frac{4\pi}{S_r l_r^2} \mathbf{I} \left[\int_0^l (x - c_1)^2 \frac{\partial \bar{a}_1}{\partial x} dx + \int_0^l (x - c_1) \bar{a}_1 dx \right]$$

$$C_{m_{\dot\alpha}} = -\frac{2}{S_r l_r^2} \int_0^l (x - c_1) \left[2\pi \mathbf{R}(\bar{a}_1 + r_0^2) - S \right] dx$$

$$C_{m_{\dot\beta}} = \frac{4\pi}{S_r l_r^2} \mathbf{I} \int_0^l (x - c_1) \bar{a}_1 dx$$

$$C_{m_{\dot p}} = -\frac{4\pi}{S_r l_r^3} \mathbf{R} \int_0^l (x - c_1)(\bar{a}_0 r_0^2 + \bar{a}_1 a_0 + \dots) dx$$

$$C_{m_{\dot q}} = -\frac{2}{S_r l_r^3} \int_0^l (x - c_1)^2 \left[2\pi \mathbf{R}(\bar{a}_1 + r_0^2) - S \right] dx$$

$$C_{m_{\dot r}} = -\frac{4\pi}{S_r l_r^3} \mathbf{I} \int_0^l (x - c_1)^2 \bar{a}_1 dx$$

$$C_{m_{\alpha p}} = \frac{8\pi}{S_r l_r^2} \mathbf{I} \int_0^l (x - c_1) \bar{a}_1 dx$$

$$C_{m_{\beta p}} = \frac{8\pi}{S_r l_r^2} \mathbf{R} \int_0^l (x - c_1) \bar{a}_1 dx$$

$$C_{m_{pp}} = \frac{4}{S_r l_r^3} \mathbf{I} \left[2\pi \int_0^l (x - c_1)(\bar{a}_0 r_0^2 + \bar{a}_1 a_0 + \dots) dx - \int_0^l (x - c_1) S \bar{\zeta}_c dx \right]$$

$$C_{m_{pq}} = \frac{4\pi}{S_r l_r^3} \mathbf{I} \int_0^l (x - c_1)^2 \bar{a}_1 dx$$

$$C_{m_{pr}} = -\frac{2}{S_r l_r^3} \int_0^l (x - c_1)^2 \left[2\pi \mathbf{R}(\bar{a}_1 - r_0^2) + S \right] dx$$

Center column:

$$C_{l_\alpha} = -\frac{4\pi}{S_r l_r} \mathbf{R} \left[(\bar{a}_0 r_0^2 + \bar{a}_1 a_0 + \dots)_{x=l} + \frac{1}{u_0} \int_0^l A_{1_0} dx \right]$$

$$C_{l_\beta} = \frac{4\pi}{S_r l_r} \mathbf{I} \left[(\bar{a}_0 r_0^2 + \bar{a}_1 a_0 + \dots)_{x=l} - \frac{1}{u_0} \int_0^l A_{1_0} dx \right]$$

$$C_{l_p} = \frac{1}{S_r l_r^2} \mathbf{R} \oint_{x=l} \frac{\partial F}{\partial p} d(\zeta \bar\zeta)$$

$$C_{l_q} = -\frac{2}{S_r l_r^2} \mathbf{R} \left[2\pi (l - c_1)(\bar{a}_0 r_0^2 + \bar{a}_1 a_0 + \dots)_{x=l} + \frac{2\pi}{u_0} \int_0^l (x - c_1) A_{1_0} dx - \int_0^l S \zeta_c dx \right]$$

$$C_{l_r} = -\frac{2}{S_r l_r^2} \mathbf{I} \left[2\pi (l - c_1)(\bar{a}_0 r_0^2 + \bar{a}_1 a_0 + \dots)_{x=l} - \frac{2\pi}{u_0} \int_0^l (x - c_1) A_{1_0} dx + \int_0^l S \zeta_c dx \right]$$

$$C_{l_{\dot\alpha}} = -\frac{2}{S_r l_r^2} \mathbf{R} \int_0^l \left[2\pi(\bar{a}_0 r_0^2 + \bar{a}_1 a_0 + \dots) - S \zeta_c \right] dx$$

$$C_{l_{\dot\beta}} = \frac{2}{S_r l_r^2} \mathbf{I} \int_0^l \left[2\pi(\bar{a}_0 r_0^2 + \bar{a}_1 a_0 + \dots) + S \zeta_c \right] dx$$

$$C_{l_{\dot p}} = \frac{1}{S_r l_r^3} \mathbf{R} \int_0^l dx \oint \frac{\partial F}{\partial p} d(\zeta \bar\zeta)$$

$$C_{l_{\dot q}} = -\frac{2}{S_r l_r^3} \mathbf{R} \int_0^l (x - c_1) \left[2\pi(\bar{a}_0 r_0^2 + \bar{a}_1 a_0 + \dots) - S \zeta_c \right] dx$$

$$C_{l_{\dot r}} = -\frac{2}{S_r l_r^3} \mathbf{I} \int_0^l (x - c_1) \left[2\pi(\bar{a}_0 r_0^2 + \bar{a}_1 a_0 + \dots) + S \zeta_c \right] dx$$

$$C_{l_{\alpha\alpha}} = \frac{8\pi}{S_r l_r} \mathbf{I} \int_0^l a_1 dx$$

$$C_{l_{\beta\beta}} = -\frac{8\pi}{S_r l_r} \mathbf{I} \int_0^l a_1 dx$$

$$C_{l_{qq}} = \frac{8\pi}{S_r l_r^3} \mathbf{I} \int_0^l (x - c_1)^2 a_1 dx$$

$$C_{l_{rr}} = -\frac{8\pi}{S_r l_r^3} \mathbf{I} \int_0^l (x - c_1)^2 a_1 dx$$

Right column:

$$C_{l_{\alpha\beta}} = -\frac{8\pi}{S_r l_r} \mathbf{R} \int_0^l a_1 dx$$

$$C_{l_{\alpha p}} = -\frac{2}{S_r l_r^2} \mathbf{I} \int_0^l \left[2\pi(\bar{a}_0 r_0^2 + \bar{a}_1 a_0 + \dots) + S \zeta_c \right] dx$$

$$C_{l_{\alpha q}} = \frac{8\pi}{S_r l_r^2} \mathbf{I} \int_0^l (x - c_1) a_1 dx$$

$$C_{l_{\alpha r}} = \frac{8\pi}{S_r l_r^2} \mathbf{R} \int_0^l (x - c_1) a_1 dx$$

$$C_{l_{\beta p}} = -\frac{2}{S_r l_r^2} \mathbf{R} \int_0^l \left[2\pi(\bar{a}_0 r_0^2 + \bar{a}_1 a_0 + \dots) - S \zeta_c \right] dx$$

$$C_{l_{\beta q}} = -\frac{8\pi}{S_r l_r^2} \mathbf{R} \int_0^l (x - c_1) a_1 dx$$

$$C_{l_{\beta r}} = \frac{8\pi}{S_r l_r^2} \mathbf{I} \int_0^l (x - c_1) a_1 dx$$

$$C_{l_{pq}} = -\frac{2}{S_r l_r^3} \mathbf{I} \int_0^l (x - c_1) \left[2\pi(\bar{a}_0 r_0^2 + \bar{a}_1 a_0 + \dots) + S \zeta_c \right] dx$$

$$C_{l_{pr}} = \frac{2}{S_r l_r^3} \mathbf{R} \int_0^l (x - c_1) \left[2\pi(\bar{a}_0 r_0^2 + \bar{a}_1 a_0 + \dots) - S \zeta_c \right] dx$$

$$C_{l_{qr}} = \frac{8\pi}{S_r l_r^3} \mathbf{R} \int_0^l (x - c_1)^2 a_1 dx$$

Note: Infinite series indicated is in all cases $\bar{a}_0 r_0^2 + \bar{a}_1 a_0 + \dfrac{\bar{a}_2 a_1}{r_0^2} + \dfrac{\bar{a}_3 a_2}{r_0^4} + \dfrac{\bar{a}_4 a_3}{r_0^6} + \dots$

Page intentionally left blank

TABLE II.- RELATIONSHIPS AMONG THE STABILITY DERIVATIVES

$$C_{Y_{pr}} = -C_{L_{pq}} = \frac{1}{2}C_{n_{\beta p}} = \frac{1}{2}C_{m_{\alpha p}} = -\frac{1}{2}C_{l_{\alpha q}} = -C_{n_{\dot\alpha}} = -\frac{1}{2}C_{l_{\beta r}} = C_{m_{\dot\beta}} = C_{L_{\dot r}} = C_{Y_{\dot q}}$$

$$C_{Y_{\beta p}} = C_{L_{\alpha p}} = C_{l_{\alpha\alpha}} = -C_{l_{\beta\beta}} = 2C_{L_{\dot\beta}} = 2C_{Y_{\dot\alpha}}$$

$$C_{n_{\alpha p}} = -C_{m_{\beta p}} = -C_{l_{\alpha r}} = C_{l_{\beta q}}$$

$$C_{n_{pr}} = -C_{m_{pq}} = \frac{1}{2}C_{l_{qq}} = -\frac{1}{2}C_{l_{rr}} = C_{n_{\dot q}} = C_{m_{\dot r}}$$

$$C_{Y_q} = C_{L_r} = -\left(\frac{l-c_1}{l_r}\right)C_{L_\beta} = \left(\frac{l-c_1}{l_r}\right)C_{Y_\alpha}$$

$$C_{Y_{\dot r}} = C_{n_{\dot\beta}} = -C_{L_{pr}}$$

$$C_{Y_{\alpha p}} = -C_{L_{\beta p}} = -C_{l_{\alpha\beta}}$$

$$C_{L_{\dot q}} = C_{Y_{pq}} = -C_{m_{\dot\alpha}}$$

$$C_{Y_{\dot r}} = C_{n_{\dot\beta}} = -C_{L_{pr}}$$

$$C_{L_q} = \left(\frac{l-c_1}{l_r}\right)C_{L_\alpha}; \qquad C_{Y_r} = -\left(\frac{l-c_1}{l_r}\right)C_{Y_\beta}$$

$$C_{Y_{\dot q}} = C_{L_{\dot r}}; \qquad C_{n_\alpha} = -C_{m_\beta}; \qquad C_{n_q} = C_{m_r}; \qquad C_{Y_{pp}} = -2C_{l_{\beta p}}$$

$$C_{L_{pp}} = 2C_{l_{\alpha p}}; \qquad C_{n_{pp}} = -2C_{l_{pr}}; \qquad C_{m_{pp}} = -2C_{l_{pq}}; \qquad C_{m_{\dot q}} = C_{n_{pq}}$$

$$C_{m_q} + C_{m_{\dot\alpha}} = -\left(\frac{l-c_1}{l_r}\right)^2 C_{L_\alpha}; \qquad C_{m_r} - C_{m_{\dot\beta}} = \left(\frac{l-c_1}{l_r}\right)^2 C_{L_\beta} = C_{n_q} + C_{n_{\dot\alpha}}$$

$$C_{n_r} - C_{n_{\dot\beta}} = \left(\frac{l-c_1}{l_r}\right)^2 C_{Y_\beta}; \qquad C_{L_{\dot\alpha}} = C_{m_\alpha} + \left(\frac{l-c_1}{l_r}\right)C_{L_\alpha}$$

$$C_{Y_{\dot\alpha}} = C_{n_\alpha} + \left(\frac{l-c_1}{l_r}\right)C_{Y_\alpha} = -C_{L_{\dot\beta}}; \qquad C_{Y_{\dot\beta}} = C_{n_\beta} + \left(\frac{l-c_1}{l_r}\right)C_{Y_\beta}$$
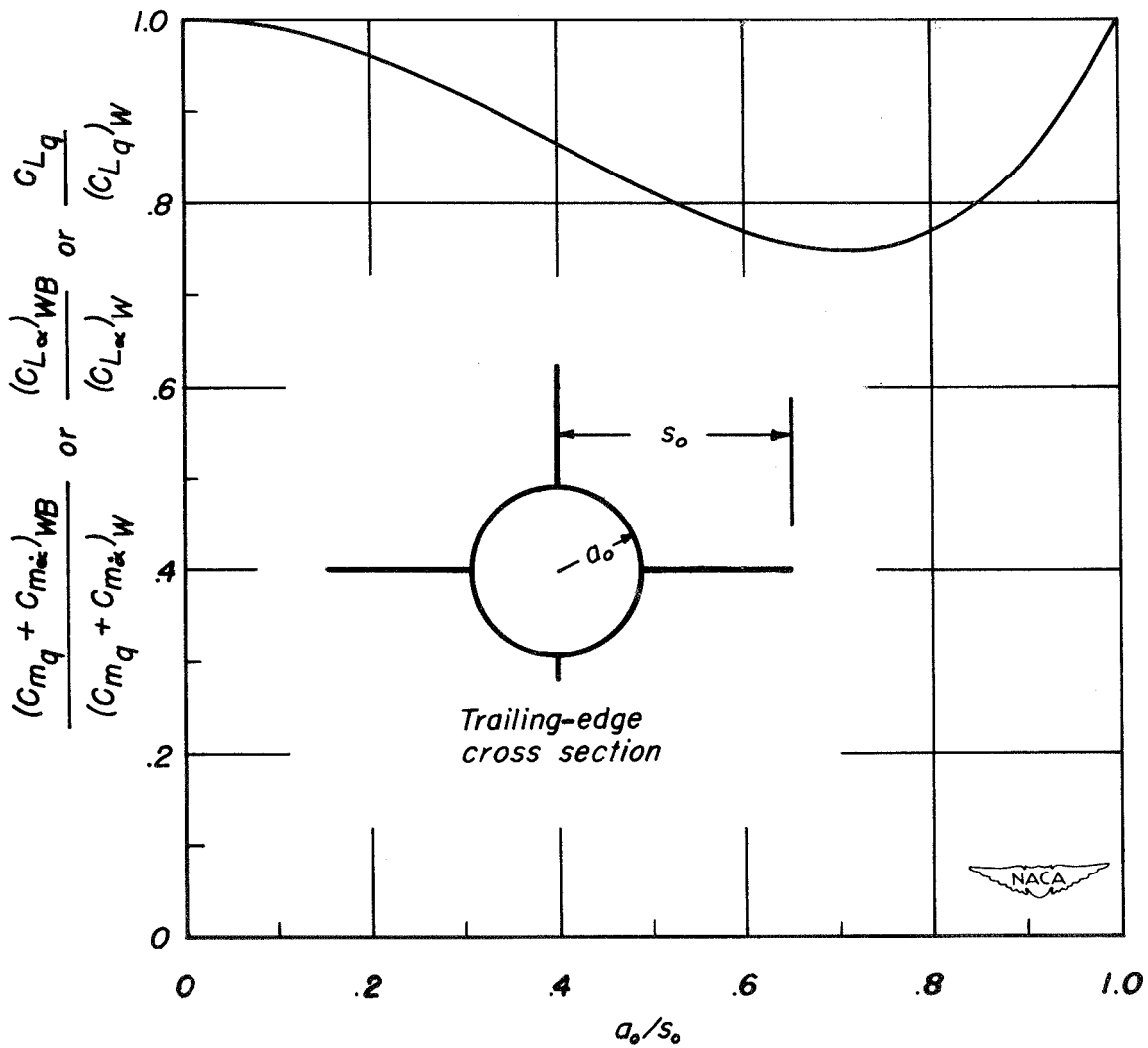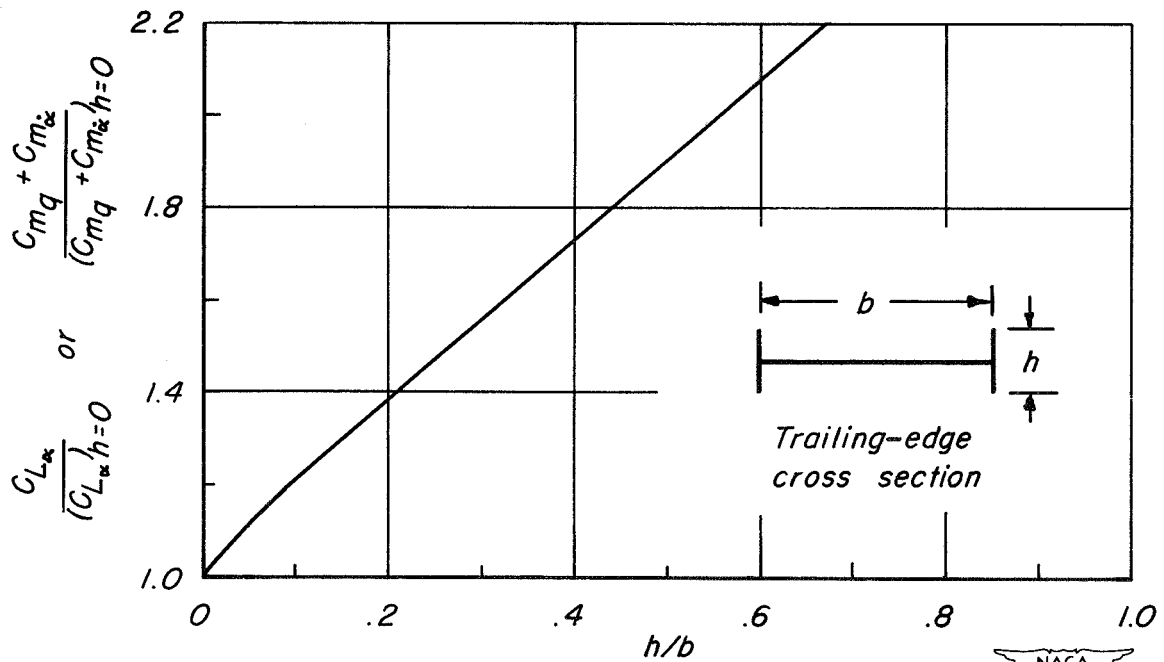
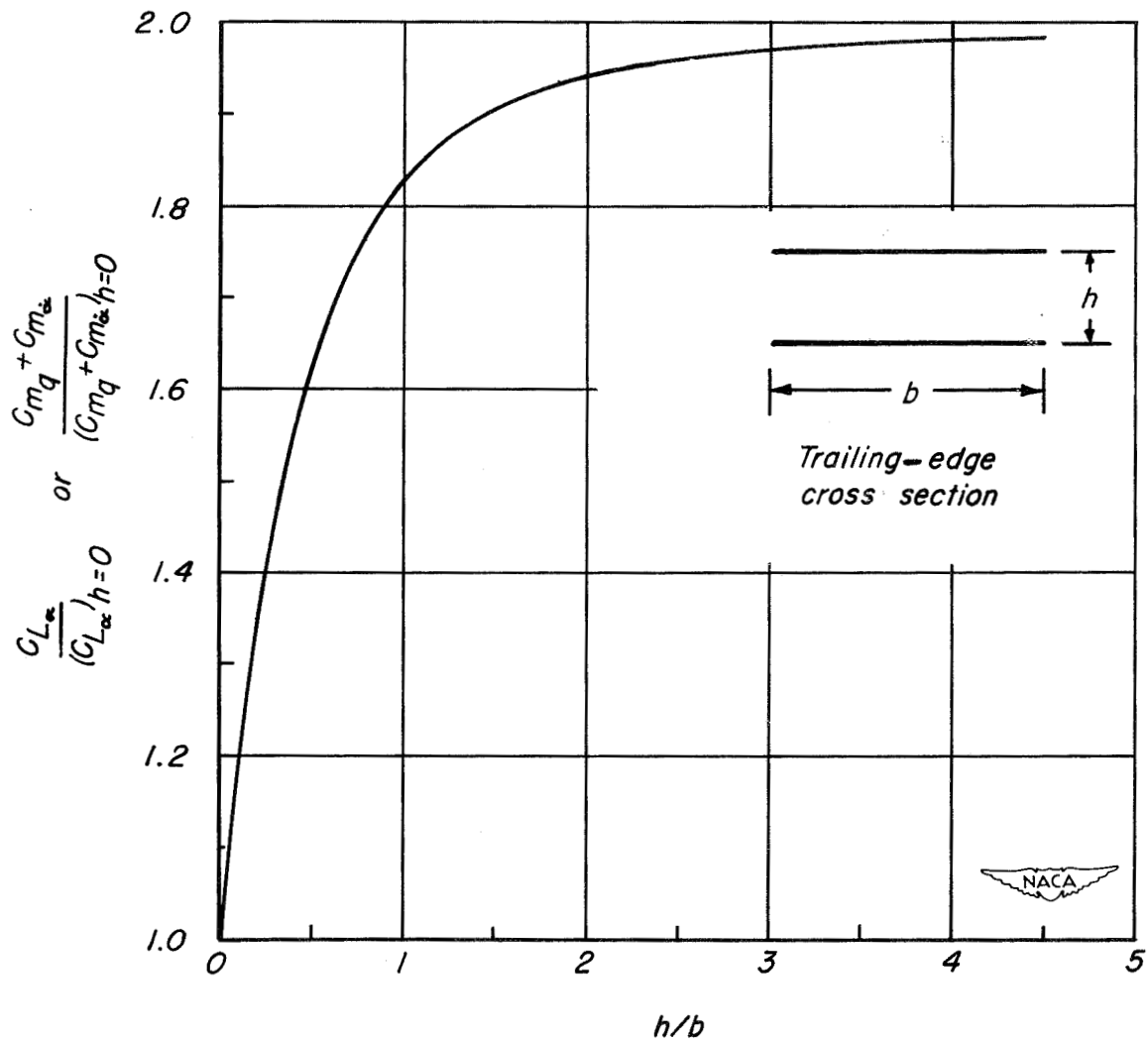Figure 1. — Damping-in-pitch for wing-body-vertical-fin combination.
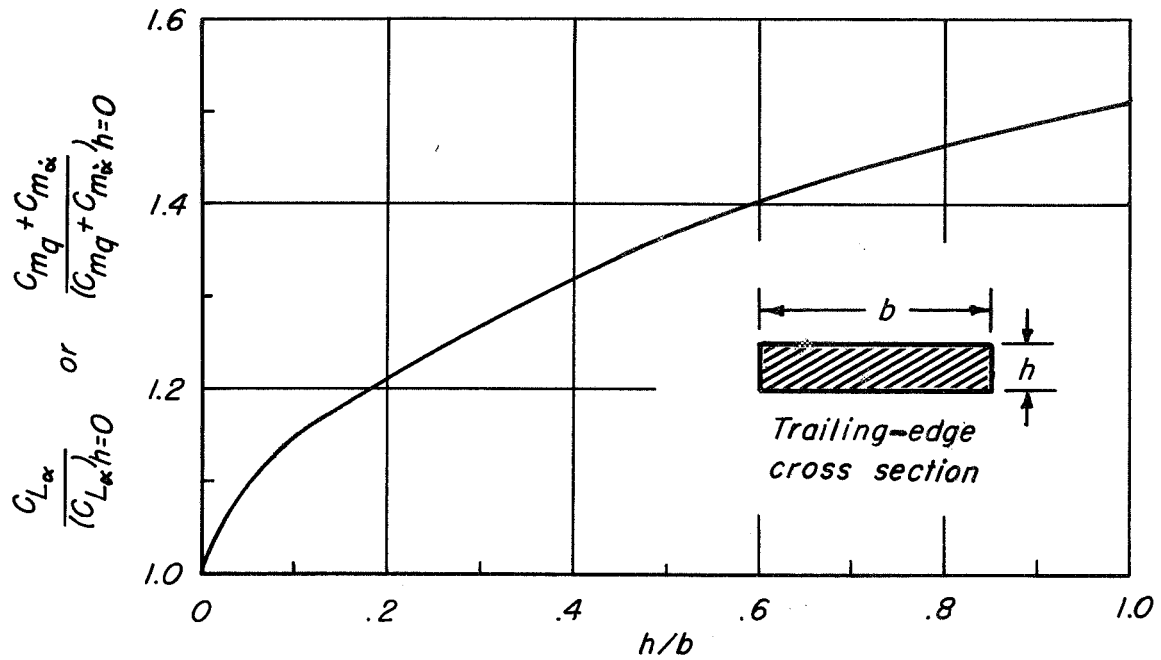
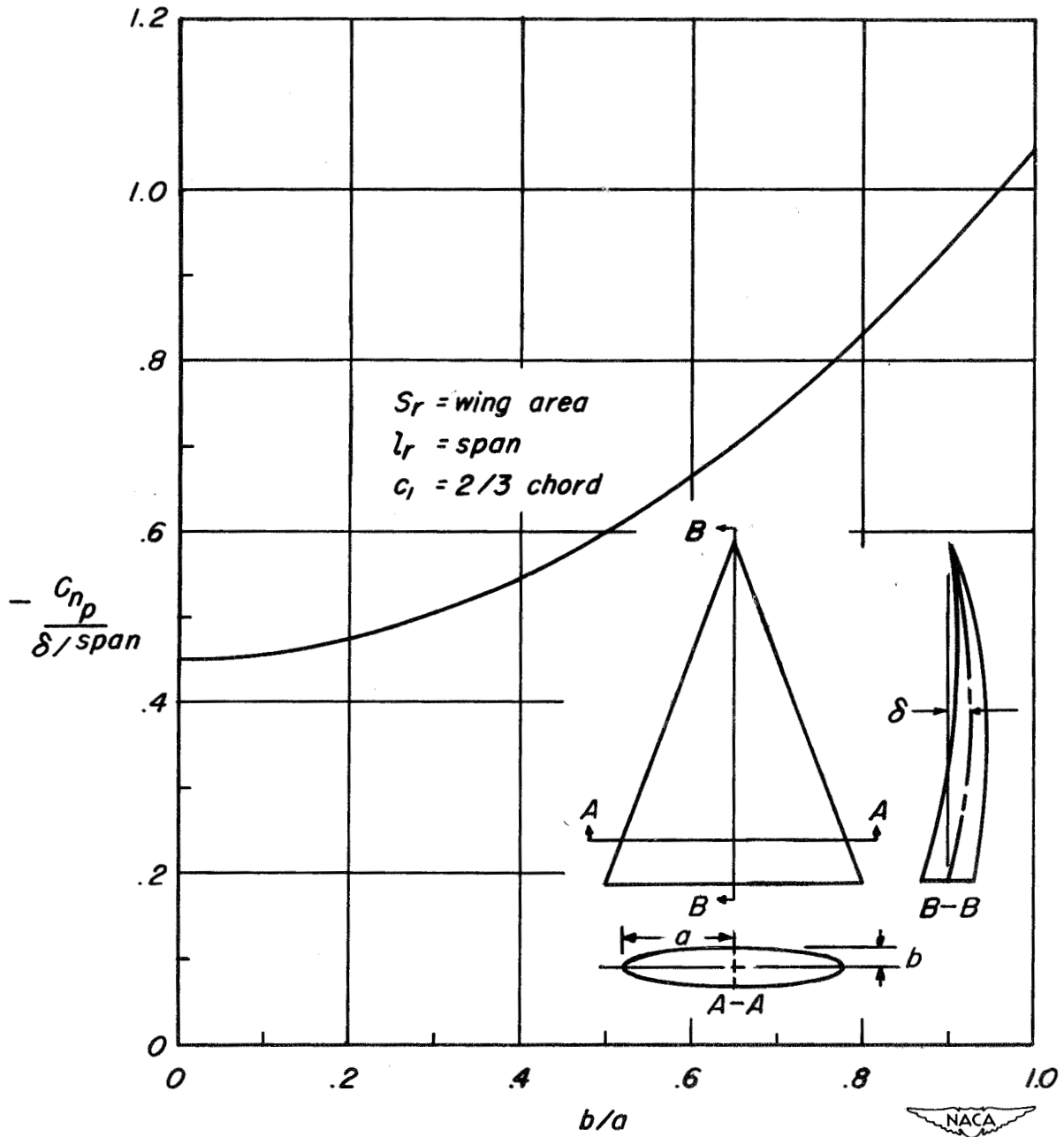(a) Blunt trailing edge of rectangular section.

(b) Wing with end plates.

Figure 2.— Damping-in-pitch and lift curve slopes for
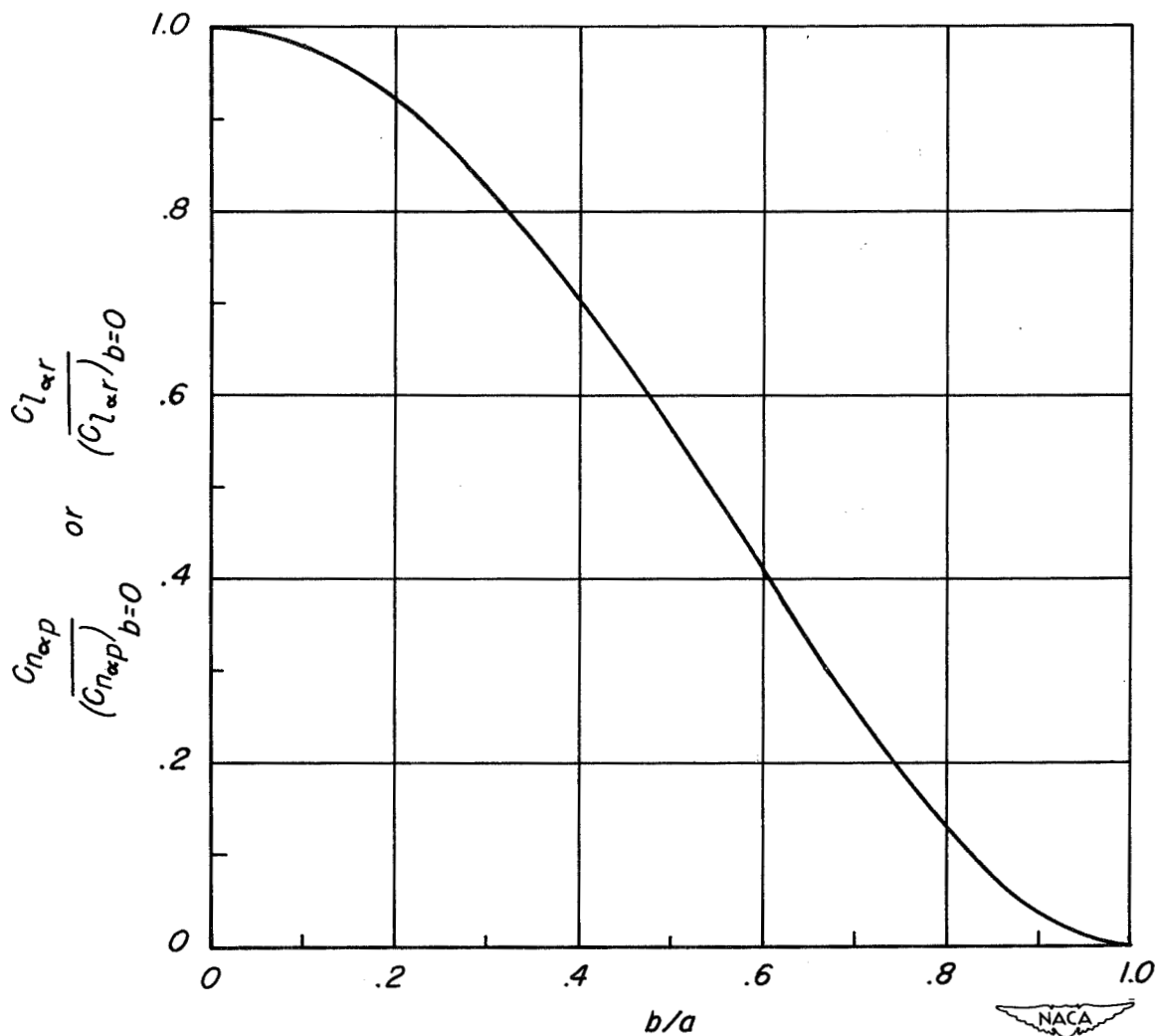several trailing edge cross sections.
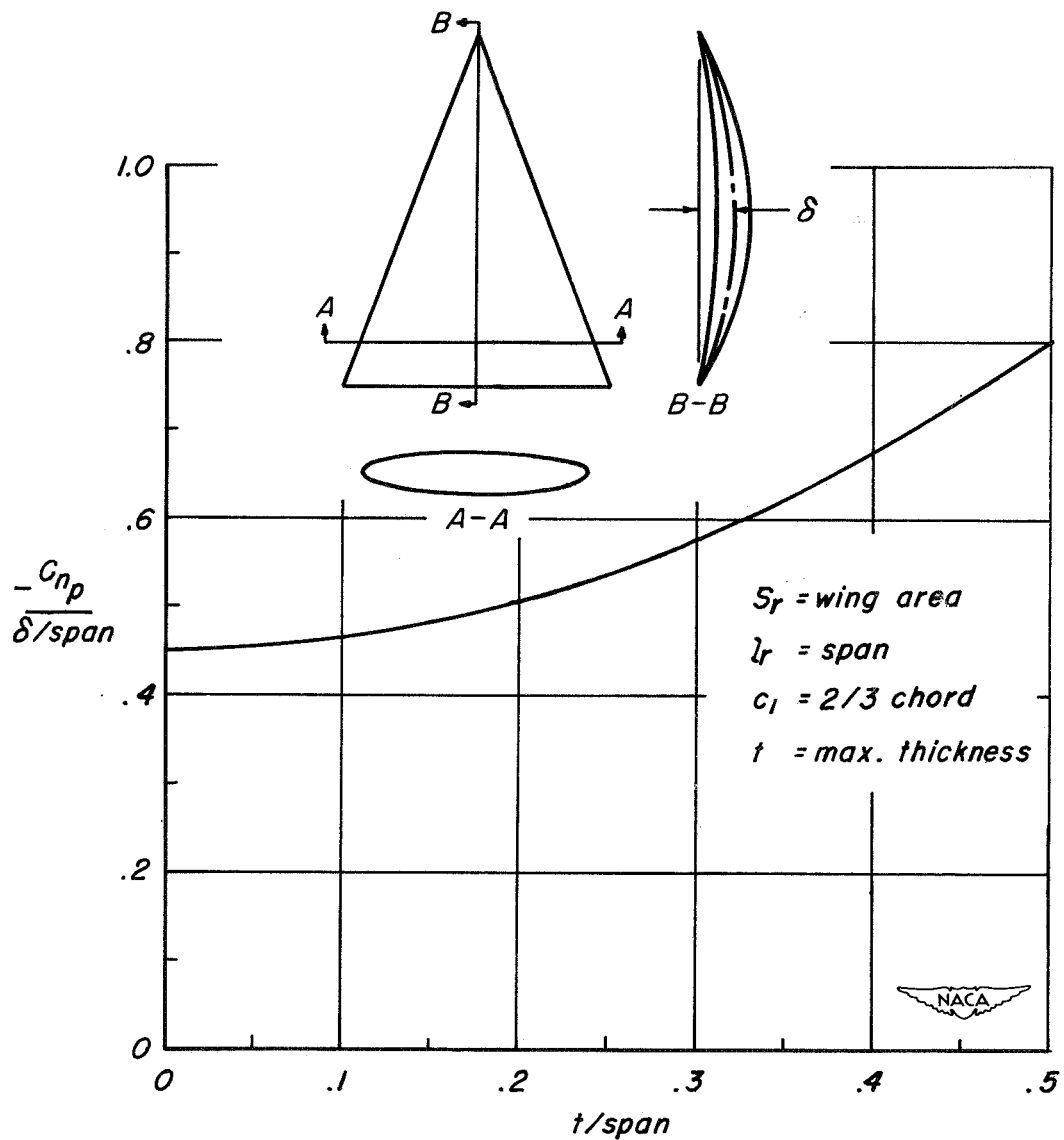
(c) Slender biplane.

Figure 2.- Concluded .

(a) Yawing moment due to rolling at zero angle of attack.

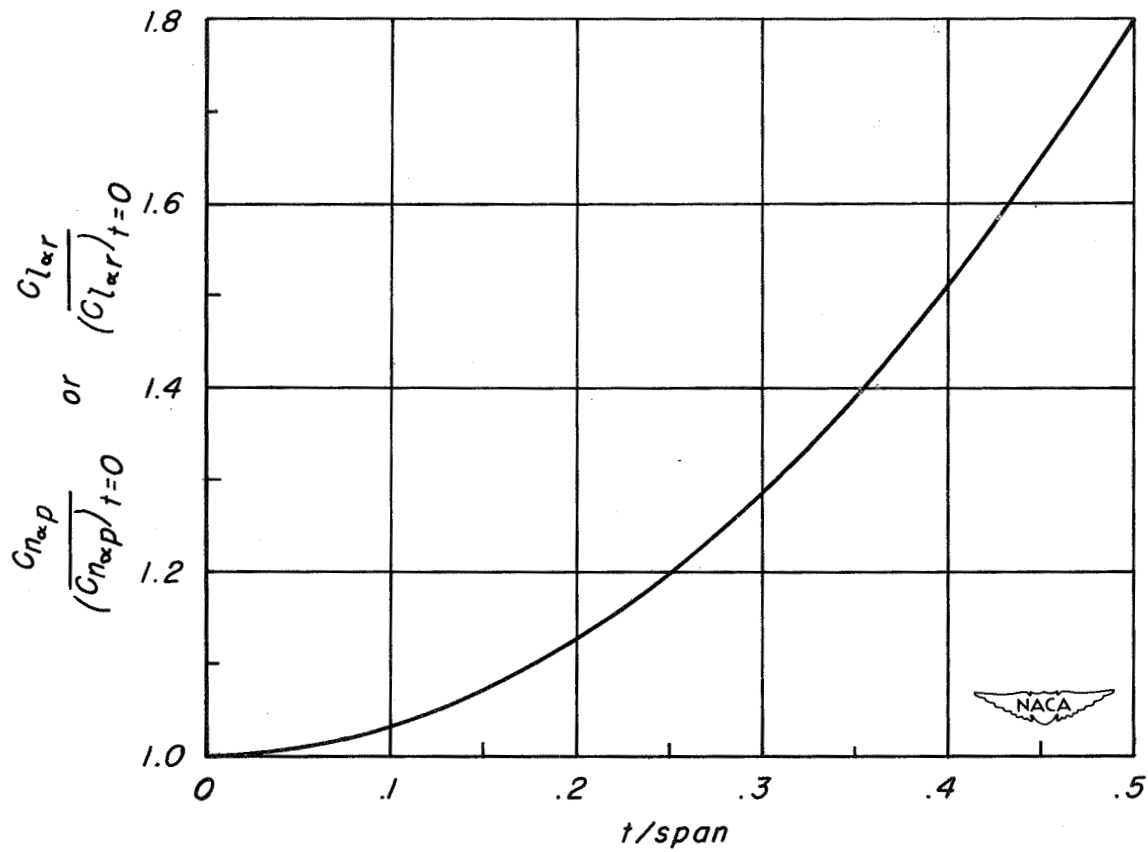Figure 3.— Effect of camber and thickness for blunt-trailing-edge triangular wing (elliptic cone).

(b) Angle-of-attack contribution to the yawing
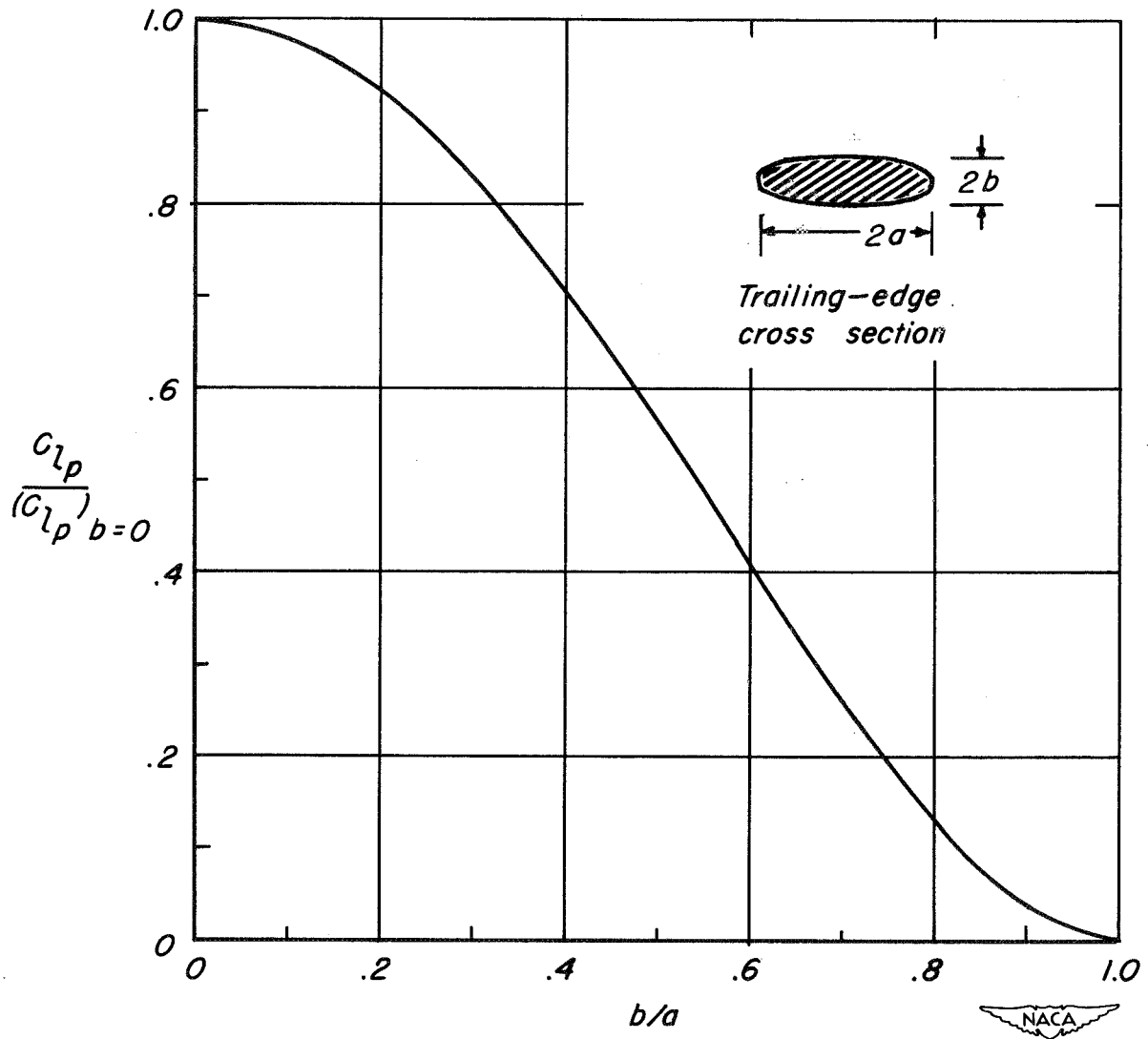moment due to rolling or the rolling
moment due to yawing .

Figure 3.- Concluded .

$$-\frac{C_{n_p}}{\delta/span}$$

S_r = wing area

l_r = span

c_l = 2/3 chord

t = max. thickness

t/span

(a) Yawing moment due to rolling at zero angle of attack.

Figure 4.— Effect of camber and thickness for sharp - trailing - edge triangular wing (Squire wing).

(b) Angle - of - attack contribution to the yawing moment due to rolling or the rolling moment due to yawing .

Figure 4.- Concluded .

Figure 5.- Effect of thickness on damping in roll for blunt - trailing - edge wing having elliptic cross section at the trailing edge.
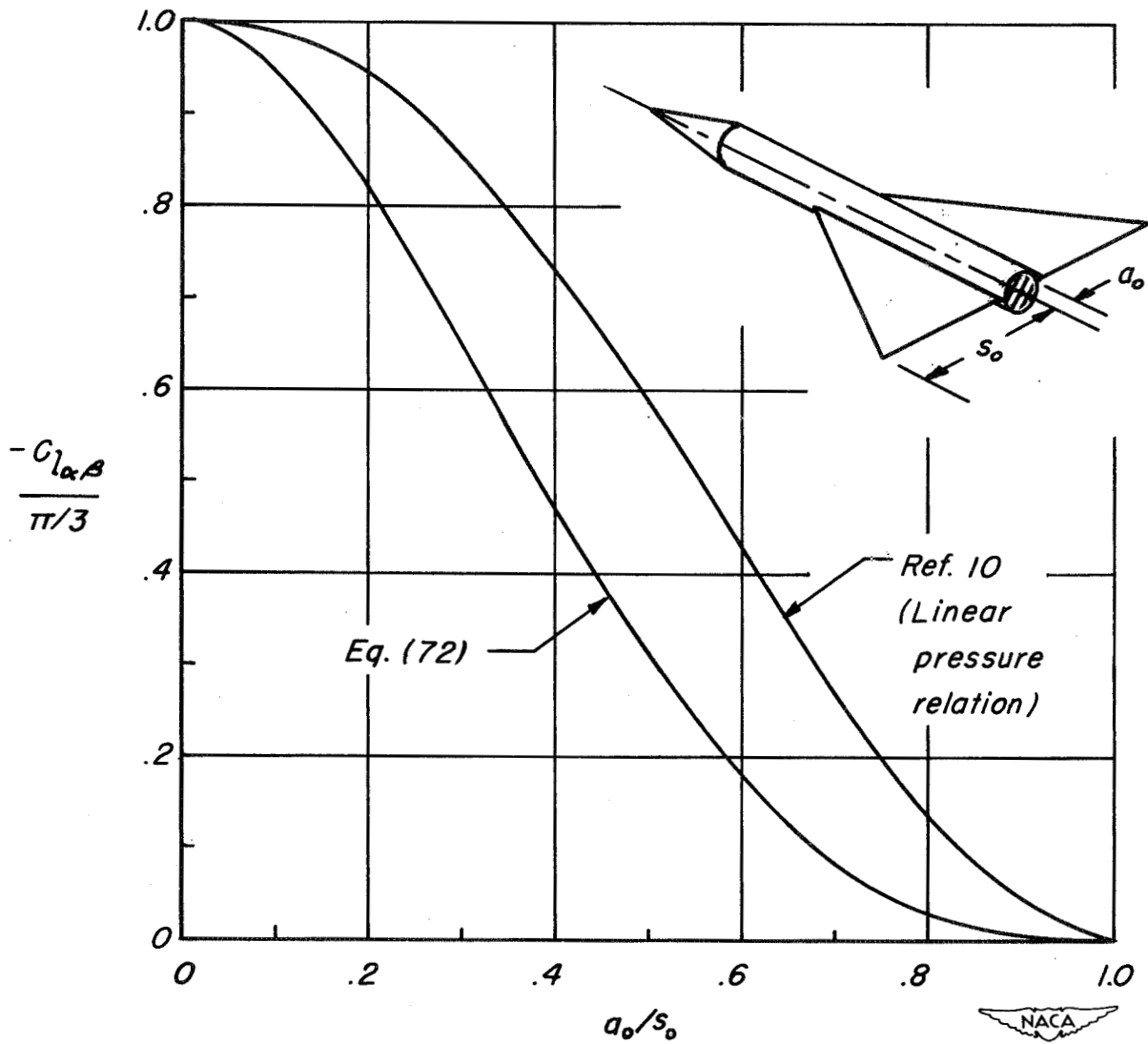
Figure 6. — Influence of the squared terms in the
pressure relation on calculations of the
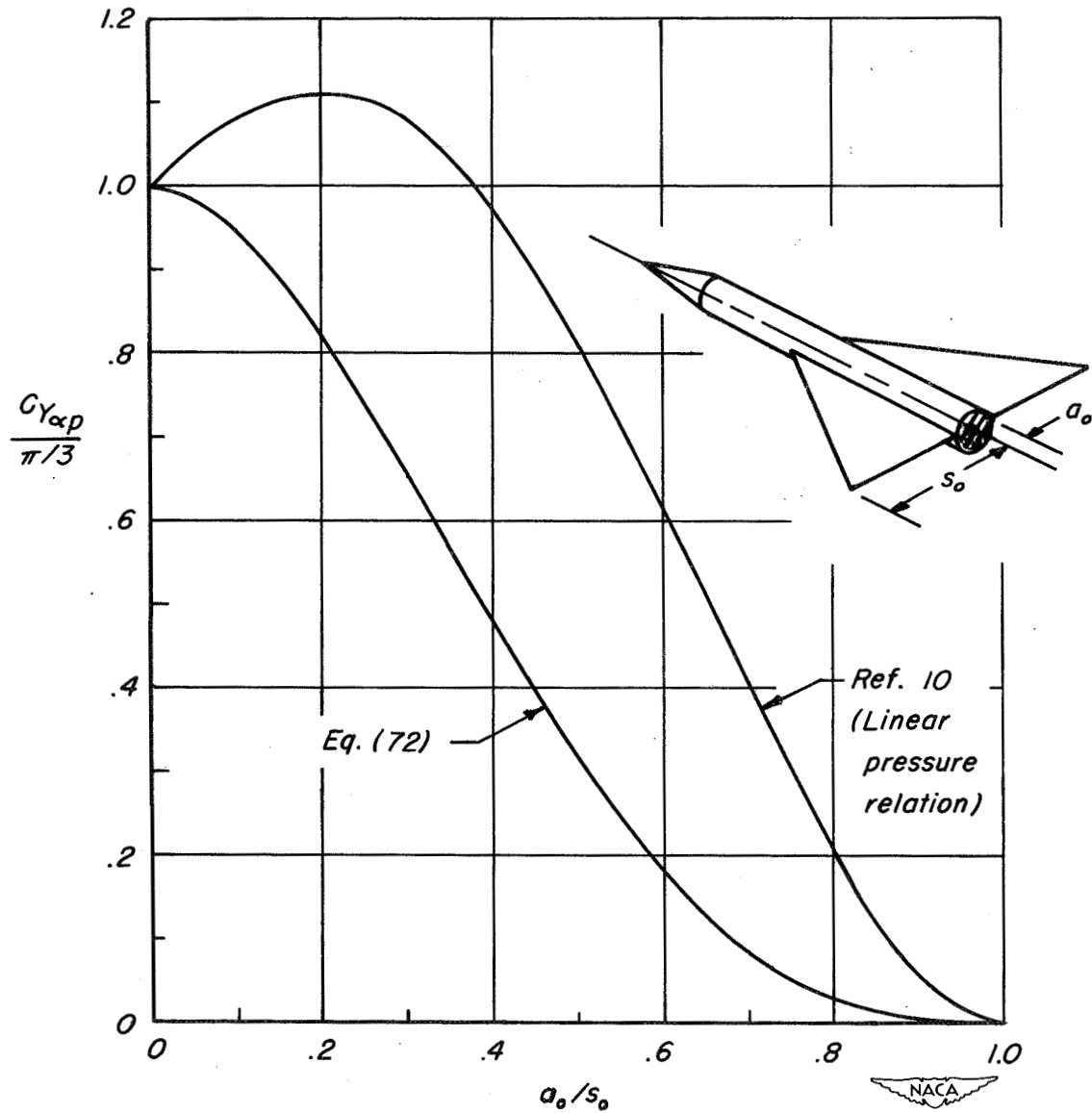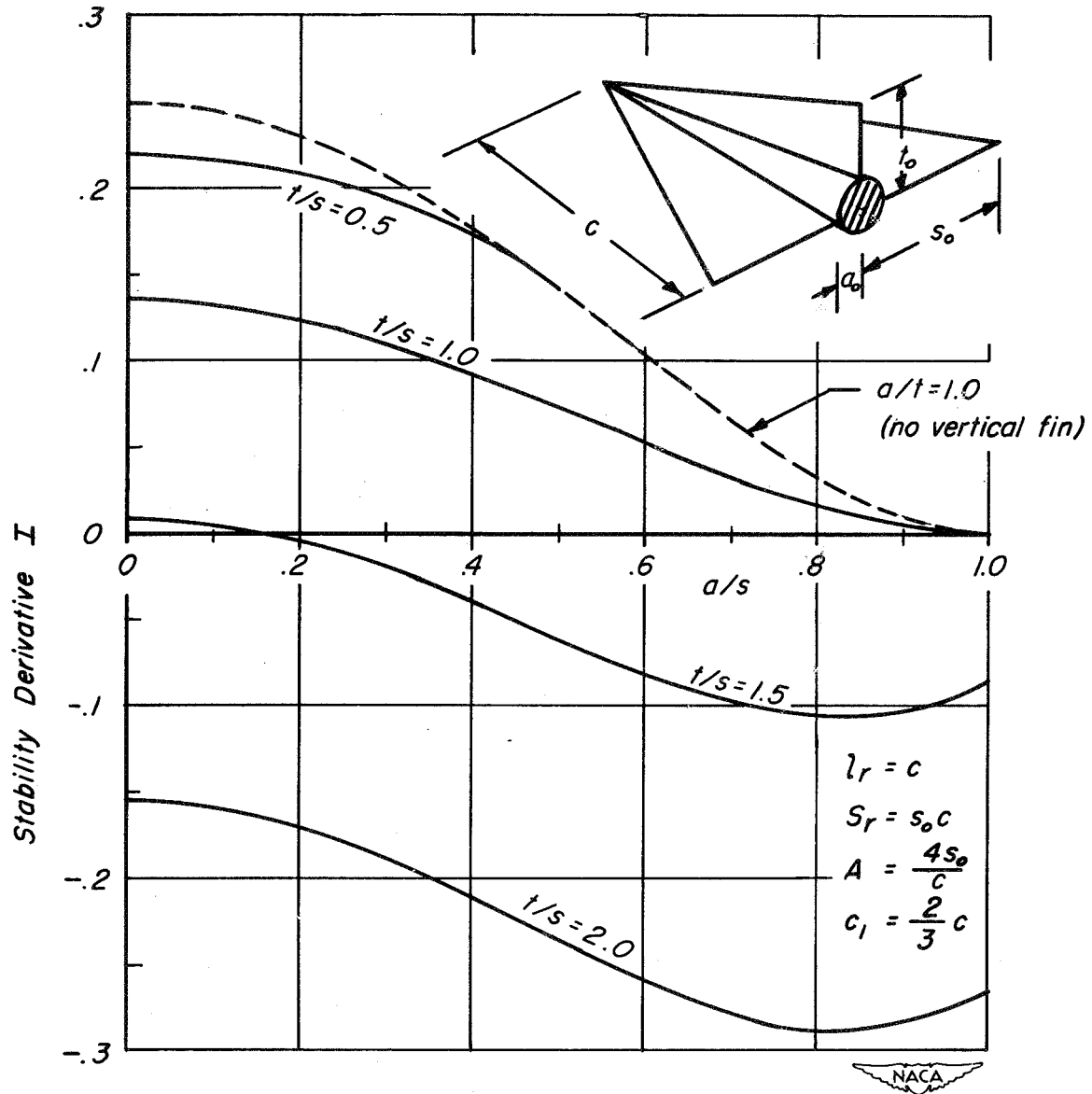rolling moment due to sideslip.

Figure 7. — Influence of the squared terms in the
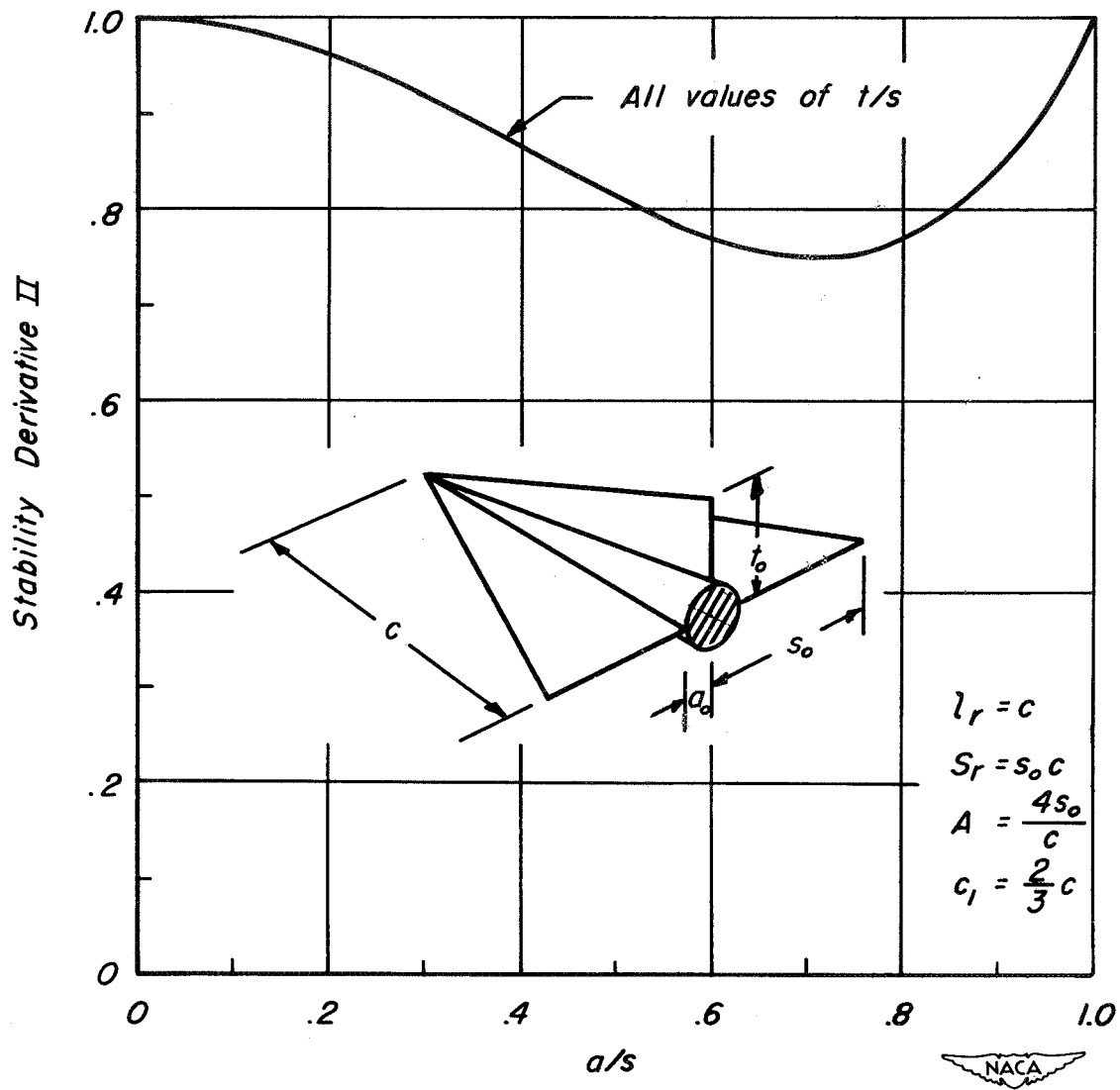pressure relation on calculations of the
side force due to rolling.

(a) Stability derivative I.

$$I = \frac{C_{Y_{\alpha p}}}{\frac{2\pi}{3}A} = \frac{-C_{n_{\alpha p}}}{\frac{\pi}{18}A} = \frac{C_{l_{qr}}}{\frac{4\pi}{135}A} = \frac{C_{m_{\beta p}}}{\frac{\pi}{18}A} = \frac{C_{l_{\alpha r}}}{\frac{\pi}{18}A} = \frac{-C_{l_{\beta q}}}{\frac{\pi}{18}A} = \frac{-C_{L_{\beta p}}}{\frac{2\pi}{3}A} = \frac{-C_{l_{\alpha \beta}}}{\frac{2\pi}{3}A}$$
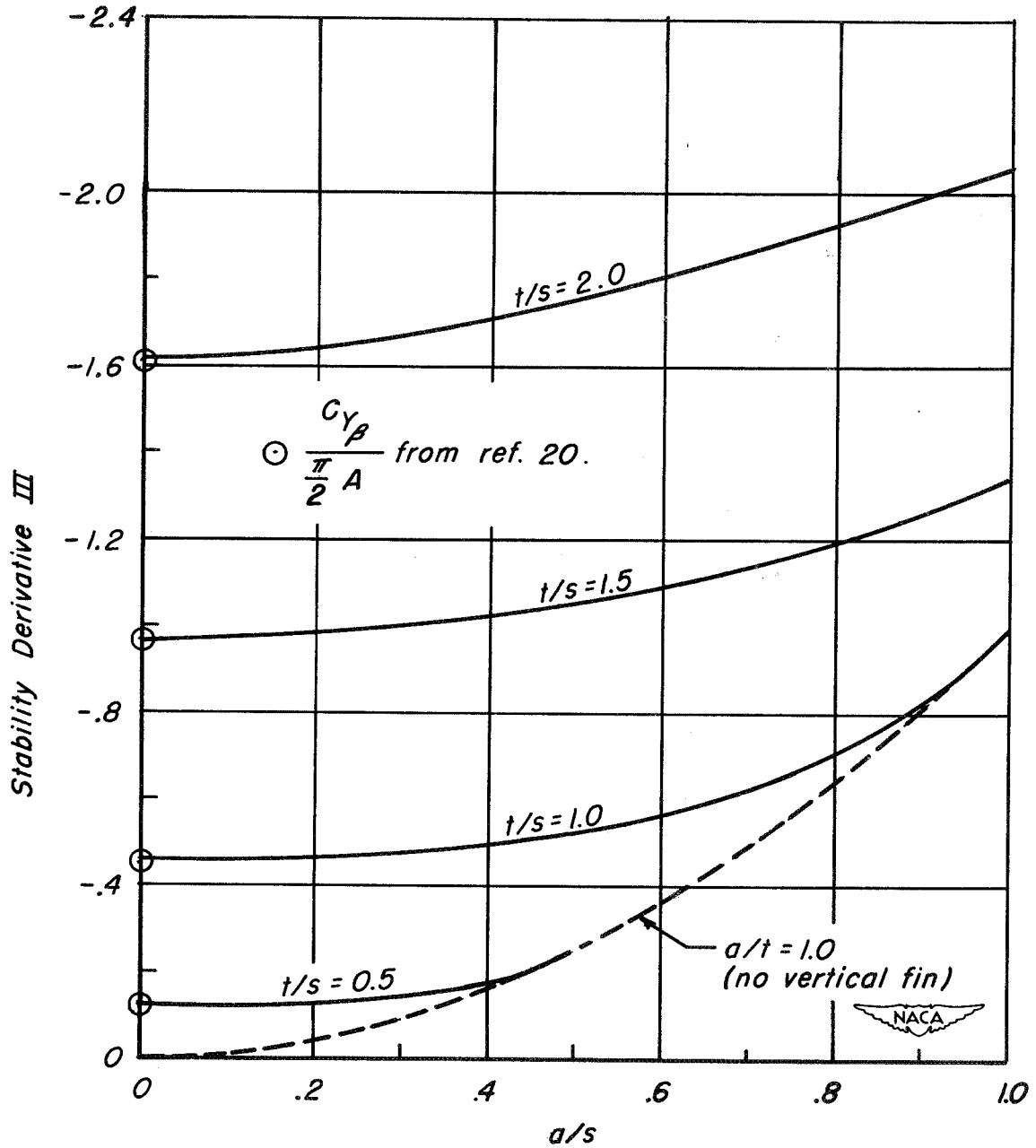
Figure 8. — Stability derivatives for conical wing-body-vertical-fin configuration.

All values of t/s

$l_r = c$

$S_r = s_o c$

$A = \dfrac{4s_o}{c}$

$c_l = \dfrac{2}{3}c$

(b) Stability derivative II.

$$II = \frac{C_{L_\alpha}}{\frac{\pi}{2}A} = \frac{C_{L_q}}{\frac{\pi}{6}A} = \frac{C_{L_{\dot\alpha}}}{\frac{\pi}{6}A} = \frac{C_{L_{\dot q}}}{\frac{\pi}{72}A} = \frac{-C_{m_{\dot\alpha}}}{\frac{\pi}{72}A} = \frac{-C_{m_q}}{\frac{\pi}{24}A} = \frac{-C_{m_{\dot q}}}{\frac{\pi}{135}A} = \frac{C_{Y_{pq}}}{\frac{\pi}{72}A} = \frac{-C_{n_{pq}}}{\frac{\pi}{135}A}$$

Figure 8.- Continued.

(c) Stability derivative III.

$$III = \frac{C_{Y_\beta}}{\frac{\pi}{2}A} = \frac{-C_{n_{\dot\beta}}}{\frac{\pi}{72}A} = \frac{-C_{m_{pr}}}{\frac{\pi}{135}A} = \frac{-C_{Y_r}}{\frac{\pi}{72}A} = \frac{C_{l_{pr}}}{\frac{\pi}{72}A} = \frac{-C_{Y_r}}{\frac{\pi}{6}A} = \frac{C_{n_r}}{\frac{\pi}{24}A} = \frac{C_{Y_{\dot\beta}}}{\frac{\pi}{6}A} = \frac{C_{n_{\dot r}}}{\frac{\pi}{135}A}$$
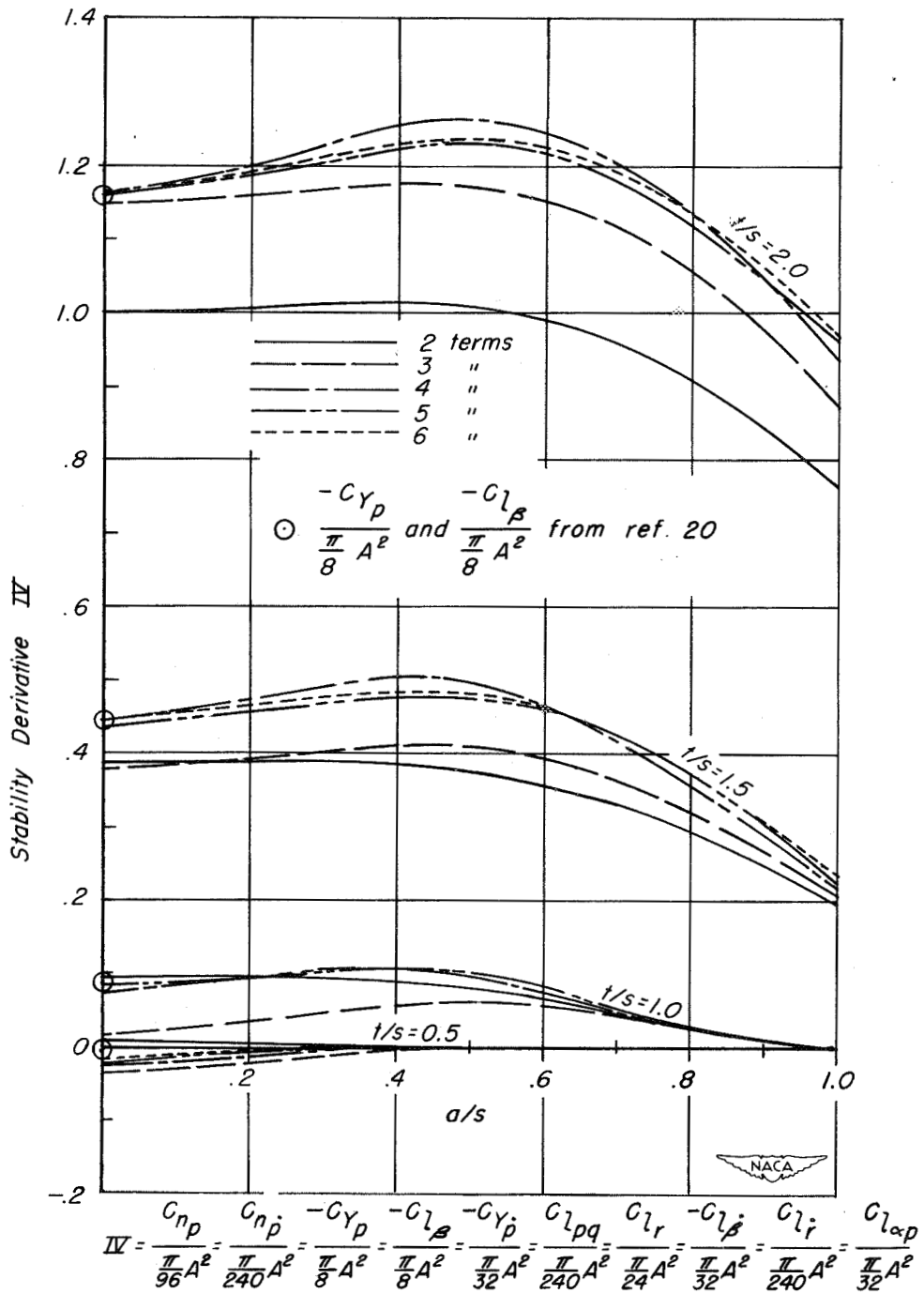
Figure 8.- Concluded .

Figure 9. — Calculation of stability derivatives for conical
wing — body — vertical — fin combination (using different
numbers of terms in infinite series of table I).